POPULATION AND COMMUNITY DYNAMICS OF TROPICAL RAIN FOREST CANOPY TREES

by

JAMES ROBERT KELLNER

(Under the Direction of Stephen P. Hubbell)

ABSTRACT

A challenge in tropical forest ecology has been integrating across tree life stages and spatial scales to understand the drivers of population and community dynamics. Here I use data from satellite and aircraft remote sensing to quantify population dynamics and canopy height changes throughout two lowland Neotropical rain forest landscapes. In the first section, develop an unbiased remote sensing approach to map and monitor rain forest canopy trees using high resolution satellite observations and Bayesian statistical modeling. I show using time series observations from satellite remote sensing between 2002 and 2007 for the rain forest canopy tree *Tabebuia guayacan* throughout 15.4 km^2 of tropical moist forest in Panama that precise estimation of survival, recruitment, and realized population growth is achievable using remote observations. Patterns in adult population dynamics were associated with historical land use and the frequency of canopy disturbance, and mediated by changes to rates of adult recruitment. Temporal variability in recruitment throughout the landscape indicates that regional processes are influencing adult population dynamics in rain forest canopy trees. The results demonstrate the feasibility of making remote measurements of canopy tree population dynamics throughout large areas, including measurement of demographic rates that are not obtainable in the field.

In a separate study I combine LiDAR remote sensing with field measurements of canopy height to quantify the structure and dynamics of an old-growth Neotropical rain forest in the

Atlantic lowlands of Costa Rica. Persistent disturbance figures prominently in the dynamics of this forest. Forty-one percent of the old-growth landscape had net canopy height changes ≥ 5 m during 8.5 years. Most gaps in the forest canopy were small, and individual gap sizes and neighbor distances followed power-laws with slopes that were indistinguishable between years. Gap sizes were unbiased with respect to topographic slope and soil Phosphorus. Despite substantial dynamics, the analysis demonstrates consistency in characteristics of forest disturbance at large spatial scales, and suggests that changes in canopy height were very close to the steady-state equilibrium expectation. These findings challenge the view that Neotropical forests are undergoing structural degradation in response to global changes, and provide evidence of the necessary conditions for selection for long-distance dispersal.

INDEX WORDS: Barro Colorado Island, Costa Rica, canopy gap, community ecology, demography, hyperspectral, La Selva Biological Station, LiDAR, Panama, population dynamics, remote sensing, *Tabebuia guayacan*, tropical rain forest

POPULATION AND COMMUNITY DYANMICS OF TROPICAL RAIN FOREST CANOPY TREES

by

JAMES ROBERT KELLNER

B.S., James Cook University, Australia, 2000

M.S., Dartmouth College, 2005

A Dissertation Submitted to the Graduate Faculty of The University of Georgia in Partial Fulfillment of the Requirements for the Degree

DOCTOR OF PHILOSOPHY

ATHENS, GEORGIA

2008

POPULATION AND COMMUNITY DYNAMICS OF TROPICAL RAIN FOREST CANOPY TREES

by

JAMES ROBERT KELLNER

Major Professor: Stephen P. Hubbell

Committee: David B. Clark
Lisa A. Donovan
Marguerite Madden
Christopher Peterson

Electronic Version Approved:

Maureen Grasso
Dean of the Graduate School
The University of Georgia
May 2008

DEDICATION

To my mother, Nancy J. Kellner, and my father, Robert A. Kellner.

ACKNOWLEDGEMENTS

I am grateful to my Ph.D. advisor, Steve Hubbell, who generously shared his ideas and time, provided critical feedback, and encouraged me to pursue my interests. David Clark, of the University of Missouri-St. Louis and La Selva Biological Station has been an important mentor and advocate of my work, and an excellent and generous collaborator. This dissertation would not have been possible without the strong support and encouragement from my beloved wife, Jillian Emmons. I am thankful to the remainder of my Ph.D. committee: Lisa Donovan, Marguerite Madden, and Chris Peterson. I would also like to thank other members of the Department of Plant Biology for facilitating my transition to Georgia: the late Bruce Haines, Jim Hamrick, Michelle Momany, Sheila Jackson, David Porter, Gregory Schmidt, and Susan Watkins. I am grateful to Marguerite Madden, the Department of Geography, and CRMS for access to high-quality computing resources and office space. I would like to thank my lab mates Yu-yun Chen, Liza Comita, Luis Borda de Agua, Jeff Lake, Monica Poelchau, and Rachel Spigler. I would also like to thank Stephanie Bohlman, Mark Brender, Caroline Colvin, Sven Cowen, W. B. Emmons, Ned Gardiner, Tommy Jordan, Brock McCarty, Helene Muller-Landau, Sean Lowrey, Aafke Oldenbeuving, David Peart, Alan Poole, Dov Sax, Shanon Shattuck, Brett Thomassie, Diane Wickland, and Joe Wright. The *Tabebuia* project was funded by grants from the NSF to Steve Hubbell. LiDAR acquisition for La Selva was funded by grants from the NSF to David Clark and separately to Elizabeth Losos and colleagues, by the TEAM project of Conservation International, made possible with funding from the Gordon and Betty Moore Foundation, and by contributions from individual researchers at the University of Maryland (Ralph Dubayah) and the University of Alberta (Arturo Sanchez). My dissertation was supported in part by a Doctoral Dissertation Improvement Grant from the NSF. I am grateful to

the Department of Plant Biology and The University of Georgia for travel assistance and final-year support. Additional support was provided by the International Biogeography Society and the American Society for Photogrammetry and Remote Sensing.

TABLE OF CONTENTS

Page

LIST OF TABLES

Page

LIST OF FIGURES

Page

CHAPTER 1

INTRODUCTION AND LITERATURE REVIEW

One of the major challenges in tropical forest ecology has been integrating across life stages and spatial scales to understand the physical and biotic drivers of population and community dynamics. Inferences about the importance of life-history tradeoffs, and of seed to-seedling density dependence ultimately depend on their ability to regulate populations of reproductive adult trees (Clark & Clark 1992; Harms *et al.* 2000; Blundell & Peart 2004; Gilbert *et al.* 2006). And understanding the dynamics of tropical forest canopies throughout large areas is fundamental to understanding the diversity and evolution of forest tree species (Denslow 1980; Hubbell & Foster 1986b; Hubbell *et al.* 1999). However, the dynamics of canopy trees, and mechanisms that influence which trees will eventually recruit to the canopy, remain poorly understood (Clark & Clark 2001; Landis & Peart 2005). Ecologists have attempted to infer the dynamics of canopy tree populations from growth and mortality within earlier life stages, but recruitment to the canopy often takes at least decades, and sometimes centuries, to occur (Clark & Clark 1992, 2001). Direct measurement of survival and recruitment within canopy or adult populations has also been problematic, because impractically large areas must be inventoried to obtain adequately sized samples for most species (Condit *et al.* 2000), and the demographic rates that need to be estimated are small numbers (Condit *et al.* 1995). Consequently, although there have been many studies of dynamics of juvenile trees, it is still unclear to what extent those dynamics represent or influence adult populations on landscapes.

A fundamental premise of this dissertation is that understanding the dynamics of adult forest trees, and of individuals occupying positions in the canopy, will strengthen inferences in basic and applied tropical forest ecology. Evidence that this premise is correct comes from

classical work in plant demography. Harper (1977) showed through careful observation of complete life cycles that to understand the most important processes in the population biology of plants requires the perspective of the 'plant's-eye view'. The plant's-eye view is the world as perceived by interacting tree species. It is influenced by the sizes and types of neighbors, and by changes to the determinants of establishment, growth and survival as individuals increase in size and become reproductive. However, with respect to forest trees, our strongest inferences are from the earliest life stages alone, and we know little of the mechanisms that mark some individuals for successful recruitment to the canopy, while others fail to leave descendants. It has been challenging to align the plant's-eye view of Harper with tropical forest dynamics. This limitation is a consequence of the difficulty of sampling rare and long-lived organisms with slow dynamics at relevant spatial scales.

Remote observation of population and community dynamics

Remote sensing can facilitate mapping and monitoring of adult tree populations and canopy dynamics throughout large areas. Work over the last few years has demonstrated the power of remote observations to obtain information on physiological condition of tree canopies (Chambers *et al.* 2007), including estimates of tree nutrient and water status (Asner & Vitousek 2005; Porder *et al.* 2005; Asner 2008), measurement of the intensity of drought stress, and estimation of net primary production (Asner *et al.* 2004) and photosynthesis (Saleska *et al.* 2007). Separate studies have demonstrated the utility of spectroscopic measurements for tree species identification (Clark *et al.* 2005; Castro-Esau *et al.* 2006; Zhang 2006; Carlson *et al.* 2007; Asner 2008), and of satellite observations to estimate forest-wide tree death rates (Clark *et al.* 2004a) and crown sizes (Clark *et al.* 2004b). LiDAR observations can quantify canopy height

changes and the vertical and horizontal distribution of biomass (Drake *et al.* 2002a; Drake *et al.* 2002b; Drake *et al.* 2003; Asner *et al.* 2008). Combining these methods with demographic analyses could open new avenues in basic and applied research, but few studies have implemented remote species identification in practice, and none has used remote observations to quantify population and community dynamics throughout tropical rain forest landscapes.

Overview of the thesis

Landscape population dynamics for a rain forest canopy tree

In chapter two, I study adult population dynamics for a rain forest canopy tree using high-resolution satellite observations. *Tabebuia guayacan* (Bignoniaceae) is a model system for landscape population dynamics. A model system is an organism with characteristics that facilitate understanding a process of general interest (Vitousek 2004). *Paramecium aurelia* and *P. caudatum* are model systems in population biology, because these organisms can be cultured in large numbers under relatively simple conditions, and the dynamics of many generations can be observed on short time scales. These characteristics allowed Gause to provide one of the earliest descriptions of competitive exclusion (Gause 1934). In plant biology, *Arabidopsis thaliana* is a model system in developmental genomics and evolution, because it can be grown readily under a variety of conditions, matures large numbers of seeds rapidly, and has a relatively small genome. Many examples of general processes in population and community dynamics are known best (or only) from model systems, including metapopulation dynamics (Hanski 1998), the keystone species concept (Paine 1969), and complex population dynamics (Turchin & Taylor 1992), a point brought to my attention by Vitousek (2004). It is not surprising that most of the examples in Harper's classic text are from studies of small herbaceous perennials sown in greenhouses.

Model systems for landscape population dynamics

Tree species with conspicuous flowering, fruiting, or leaf phenology are model systems for landscape population monitoring, because large samples of canopy or adult individuals can be obtained efficiently using remote observations, overcoming sampling difficulties in the field. This is different from typical approaches to remote identification of tree species, where studies assume that an operational method must use high-performance spectroscopic measurements to discriminate between hundreds of species on the basis of optical properties of green vegetation. In my view, that approach is not always practical or necessary. Although imaging spectroscopy will continue to be essential to many of the most important applications in biophysical remote sensing (Asner 2004, 2005; Porder *et al.* 2005; Asner 2008), its potential for regular monitoring throughout large areas of the continental tropics – where capacity for mapping and monitoring is most urgently needed – is restricted, because hyperspectral sensors with high spatial resolution are confined to aircraft, and access is expensive and difficult or impossible for all but the most well-studied sites. The optical properties of green vegetation are very similar for most species, and most of the variation in spectral responses within the shortwave spectrum (400 – 2500 nm) occurs within species, not between them (Castro-Esau *et al.* 2006). In addition, complete species inventories are not required to address many questions in population and community dynamics. At issue here is not the existence or importance of questions that do require complete species inventories, but to argue that the most fundamental drivers of population and community dynamics operating at large spatial scales can probably be identified and understood using a smaller number of model organisms that can be sampled using globally accessible remotely sensed data.

Examples of tree species with model characteristics for landscape population monitoring include Bignoniaceous trees that have synchronous flowering (Janzen 1967), and species that undergo leaf senescence in response to seasonal variation. For example, reflectance of leaf and floral pigments is expressed in the visible wavelengths (400 – 700 nm), a feature that has allowed me to observe flowering status of *T. guayacan*, *Jacaranda copaia* and *Vochysia ferruginea* on Barro Colorado Island, Panama (BCI) using multispectral satellite observations from the QuickBird sensor. In Costa Rica, flowering *Dipteryx panamensis* is distinct using Ikonos satellite data at La Selva Biological Station, and *T. ochracea* is detectible within tropical dry forest in Guanacaste using observations from the QuickBird sensor. Although flowering status can be a conspicuous feature of tropical forest canopies, leaf phenology of *D. panamensis* is observable as a rust-colored hue prior to senescence on BCI. In leafless condition, individuals of any species are readily observed using hyperspectral observations, because reflectance of leafless crowns in the short-wavelength infrared (1300 – 2500 nm) is dominated by lignin, rather than water in floral tissue (Asner 1998). Thus, there are likely to be many species with characteristics that facilitate remote detection and monitoring. Studies that leverage these characteristics to define the distribution, abundance, and dynamics of canopy tree species can test novel hypotheses about population and community dynamics at large spatial scales.

Remote estimation of demographic rates

The approach in chapter two takes advantage of natural variability in spectral reflectance during synchronous annual flowering of *T. guayacan* to detect carotenoid pigments within flowering adult canopies, and uses this information to delineate individual tree crowns and generate observations of individuals through time. I analyze these observations in a Bayesian

state-space framework similar to classical capture-mark-recapture analysis (Cormack 1964; Jolly 1965; Seber 1965; Pradel 1996; Royle 2008), which decouples the latent demographic process (survival and recruitment) from the observational process (detection based on carotenoid expression) to quantify survival, recruitment, and realized population growth.

Canopy gaps and the dynamics of a Neotropical rain forest

In closed-canopy tropical rain forests, localized canopy openings occur that mediate access to light and space in the forest understory (Brokaw 1982, 1985; Hubbell & Foster 1986b). These 'canopy gaps' are caused by the death of, or damage to, a canopy-forming tree. Quantifying the sizes and spatial properties of gap distributions on landscapes is fundamental to understanding the diversity and evolution of forest tree species (Denslow 1980; Hubbell & Foster 1986b; Hubbell *et al.* 1999). For many species, gaps are essential at some stage in ontogeny for individuals to recruit to the canopy.

In chapter three, I combine LiDAR remote sensing with field measurements of canopy height to characterize the size frequency distribution, spatial characteristics, and dynamics of canopy gaps in an old-growth Neotropical rain forest in the Atlantic lowlands of Costa Rica. By recording the return-time of reflected laser pulses, LiDAR sensors acquire physically-based measurements of canopy height and ground elevation (m), and the vertical and horizontal distribution of biomass (Drake *et al.* 2002a; Drake *et al.* 2003; Clark *et al.* 2004c; Asner *et al.* 2008). They are ideal for quantifying the structure and dynamics of forest canopies, because they provide spatially referenced, extensive and finely grained vegetation height measurements that are objectively acquired. LiDAR measurements facilitate access to characteristics of forest

canopies at multiple scales, and permit objective analyses of canopy structure and dynamics on landscapes.

Potential and limitations of hyperspectral imaging to estimate upper-canopy foliar nitrogen in a lowland Neotropical rain forest

In the final data chapter, I summarize the status of an effort to estimate foliar N within tree canopies using airborne hyperspectral imaging over a tropical rain forest in the Atlantic lowlands of Costa Rica. The objectives are to describe and interpret variation in canopy N throughout a tropical rain forest landscape, and to test whether the growth and performance of individuals can be predicted using their nutrient status relative to neighbors (the hypothesis of limiting similarity, MacArthur & Levins 1967; McGill *et al.* 2006). The study encountered limitations that have thus far preempted useful estimates of canopy N to be made. Because many of these limitations may emerge at other sites, I discuss and evaluate them in detail. I conclude by arguing that the inability to obtain useful estimates of canopy N was probably caused by changes to the nutrient status and structure of the forest between the time of image acquisition and collection of field measurements, rather than inherent lack of information within the spectroscopic measurements. I point to alternative methods that have been used to retrieve canopy N from spectroscopic data in the absence of field measurements, and suggest that useful estimates of canopy N may be possible.

CHAPTER 2

LANDSCAPE POPULATION DYNAMICS IN A RAIN FOREST CANOPY TREE QUANTIFIED USING HIGH RESOLUTION SATELLITE OBSERVATIONS [1]

[1] Kellner, J.R. and S.P. Hubbell. Submitted to Proceedings of the National Academy of Sciences on March 5, 2008.

Abstract

Ecologists typically study the dynamics of tropical forests and individual tree species using mapped permanent plots of up to several tens of hectares in size, but whether these findings are representative of canopy populations on landscapes is largely unknown. We developed an unbiased remote sensing approach to map and monitor rain forest canopy trees using high resolution satellite observations and Bayesian statistical modeling. We show using time series observations from satellite remote sensing between 2002 and 2007 for the rain forest canopy tree *Tabebuia guayacan* throughout 15.4 km^2 of tropical moist forest in Panama that precise estimation of survival, recruitment, and realized population growth is achievable using remote observations. Patterns in adult population dynamics were associated with historical land use and the frequency of canopy disturbance, and mediated by changes to rates of adult recruitment. Temporal variability in recruitment throughout the landscape indicates that regional processes are influencing adult population dynamics in rain forest canopy trees. Our results demonstrate the feasibility of making remote measurements of canopy tree population dynamics throughout large areas, including measurement of demographic rates that are not obtainable in the field.

Introduction

One of the major challenges in tropical forest ecology has been integrating across life stages and spatial scales to understand the physical and biotic drivers of population and community dynamics. Inferences about the importance of life-history tradeoffs, and of seed to-seedling density dependence ultimately depend on their ability to regulate populations of reproductive adult trees (Clark & Clark 1992; Harms *et al.* 2000; Blundell & Peart 2004; Gilbert *et al.* 2006). And precisely estimating demographic rates in adult canopy tree populations is essential to making robust predictions of tropical forest change (Clark *et al.* 2003). However, the dynamics of canopy trees, and mechanisms that influence which trees will eventually recruit to the canopy, remain poorly understood (Clark & Clark 2001; Landis & Peart 2005). Ecologists have attempted to infer the dynamics of adult tree populations from growth and mortality within earlier life stages, but transitions from juvenile to adult often take at least decades, and sometimes centuries, to occur (Clark & Clark 1992, 2001). Direct measurement of adult survival and recruitment is also problematic, because impractically large areas must be inventoried to obtain adequately sized samples for most species (Condit *et al.* 2000), and the demographic rates that need to be estimated are small numbers (Condit *et al.* 1995). Consequently, although there have been many studies of dynamics of juvenile trees, it is still unclear to what extent those dynamics represent or influence adult populations on landscapes.

Satellite remote sensing may facilitate mapping and monitoring of adult tree populations throughout large areas (Clark *et al.* 2004a; Clark *et al.* 2004b). Previous work has demonstrated the utility of airborne spectroscopic measurements for tree species identification (Clark *et al.* 2005; Carlson *et al.* 2007), and of satellite observations to estimate forest-wide tree death rates

(Clark *et al.* 2004a). Although imaging spectroscopy is essential to many of the most important applications in biophysical remote sensing (Asner 2004, 2005; Porder *et al.* 2005), its potential for regular monitoring throughout large areas of the continental tropics is restricted, because sensors with high spatial resolution are confined to aircraft, and access is expensive and difficult for most regions. Estimates of tree death rates have been made using visual interpretation, and thus our ability to implement species-level demographic analysis throughout tropical rain forest landscapes has been limited. Development of capacity for widespread monitoring will require species that can be identified using globally available satellite observations, combined with automated tree-crown recognition and rigorous statistical analysis to estimate demographic rates. This will help to overcome sampling difficulties in the field, because most tropical rain forest canopy tree species occur at very low population densities (Condit *et al.* 2000), and will generate opportunities to address new questions about tropical forest dynamics at landscape to regional scales.

We developed an unbiased remote sensing approach to map and monitor adult population dynamics for a rain forest canopy tree (*Tabebuia guayacan* Bignoniaceae) using spectral mixture analysis (Adams *et al.* 1993; Roberts *et al.* 1998) and high spatial resolution satellite observations from the QuickBird and Ikonos sensors. The method takes advantage of natural variability in spectral reflectance during synchronous annual flowering to detect carotenoid pigments within flowering adult canopies, and uses this information to delineate individual tree crowns and generate observations of individuals through time (Fig. 2.1, and supporting Fig. 2.4). We analyze these observations in a Bayesian state-space framework similar to classical capture-mark-recapture analysis (Cormack 1964; Jolly 1965; Seber 1965; Pradel 1996; Royle 2008). State-space modeling decouples the latent demographic process (survival and recruitment) from

the observational process (detection based on carotenoid expression) to quantify population dynamics. Integrating tree identification and demography into a single methodological framework enabled precise estimates of demographic rates to be made over a tropical rain forest landscape.

Results and Discussion

Remote estimation of demographic rates

The population sample consisted of 690 adult trees observed on four occasions during five years throughout 15.4 km^2 of tropical moist forest on Barro Colorado Island, Panama (BCI), a mean observed density of 0.45 individuals $\cdot$ ha^{-1} (Fig. 2.2). Observed adult density was higher in second-growth forest (0.57 individuals $\cdot$ ha^{-1}), than in old-growth (0.32 individuals $\cdot$ ha^{-1}). In the 2005 field census of the 50 ha plot, mean density for *T. guayacan* $\geq$ 20 cm DBH was 0.45 individuals $\cdot$ ha^{-1}.

Realized population growth was associated with historical land use, and mediated by differences in recruitment. Adult abundance increased in old-growth forest, but was closer to replacement levels in second-growth (Fig. 2.3). Annual survival for *T. guayacan* stems $\geq$ 20 cm diameter at breast height (DBH) in the mapped 50 ha plot was 0.991. The median of the posterior distribution of annual survival obtained remotely for adult *T. guayacan* in old-growth forest was 0.987 $\pm$ 0.011 S.E., a difference between field and remotely sensed estimates of less than half a percent (Fig. 2.3). Throughout the landscape this rate was independent of historical land use (Fig. 2.3), and it varied minimally through time (Table 4). Because field and remotely sensed survival estimates were derived from independent sources, their concordance provides evidence

that unbiased, precise estimation of demographic rates for forest tree populations is achievable using satellite observations.

Although survival was relatively constant through time and varied minimally with historical land use, recruitment was more variable (Fig. 2.3). The median of posterior annual recruitment across the old-growth landscape was 0.033 ± 0.019 S.E., which was more than double the rate observed within secondary forest on BCI (0.014 ± 0.012 S.E.). Because realized population growth is influenced by the relative contributions of survival and recruitment, this indicates that variation throughout the landscape in adult population dynamics is being driven by changes in adult recruitment. This finding is significant, because adult tree recruitment has been extremely difficult to estimate precisely in the field for most species, but can now be estimated using remote observations.

Field validation carried out across BCI indicates that the sample of adult trees identified remotely is unbiased with respect to stem diameter and tree height. Using a combination of field checks and high resolution aerial photography, we detected one misidentification error in all 1087 observations for 690 unique individuals. Errors in crown delineation occurred in 21 trees, and all errors were corrected manually prior to analysis. Taken together, sources of error may influence up to 3.5% of trees in our sample (see supporting information, and Figs. 6 – 7).

Validation

We observed 690 unique *T. guayacan* in 380, 303, 331, and 75 individual detection events in 2002, 2004, 2006 and 2007 respectively (Fig. 1). There were 17, 3, 284, and 165 individuals that were censored by cloud cover in 2002, 2004, 2006 and 2007 respectively. Thirty-six trees were censored in two different years, and 4 trees were censored in three years. No trees checked in the

field that were identified using satellite observations belonged to other species. However, one tree that was detected in 2006, but not checked in the field, appeared using 0.08 m aerial photographs to be the crown of a semi-deciduous *Dipteryx panamensis* Fabaceae, which we omitted from our sample. Crowns of some *D. panamensis* experience a rust-colored hue prior to leaf drop (J. Kellner, personal observation). We searched for additional misidentification errors in our data using 0.08 m aerial photography from 2005 and 2007 that was collected during *T. guayacan* flowering. No additional misidentifications were detected. We conclude that the rate of misidentification errors is ≈ 1 in 1087 (i.e. 1 / [380 + 303 + 331 + 75 + 1]).

Field checks and visual examination of aerial photography and satellite images revealed four cases where two individual trees were segmented as a single object in 2002 and 2004, and two cases in 2006. There was one case in 2006 where three individual trees were segmented as a single object. No errors of this type occurred in 2007. Because most adult *T. guayacan* do not have conspecific neighbors, the potential for this error to occur is minimized. We manually corrected each error and updated encounter histories prior to statistical analysis. Taken together, combined errors in species identification and crown delineation may influence up to 8 (trees in 2002) + 8 (trees in 2004) + 4 (trees in 2006) + 3 (trees in 2006) + 1 (false positive in 2006) = 24 trees. This corresponds to 24 / 690 = 3.5% of the trees in our sample.

We conducted field checks on 167 trees throughout the BCI forest, including 110 ground reference individuals, and 57 trees detected first by satellite. Out of the 110 ground reference trees, 90 (82%) had also been detected at least one time using satellite observations. Comparison of trees that were detected by satellite to trees in the ground reference sample indicates that the

sample obtained remotely is unbiased with respect to stem diameter and tree height ($P = 0.576$ and $P = 0.832$, respectively, Fig. 7). Indeed, the smallest stem observed was detected by satellite observations in 2002 and 2006 (a 24.3 cm diameter adult in old-growth forest).

Potential drivers of landscape population dynamics

Variability throughout the landscape in adult population dynamics is consistent with the life history of *T. guayacan*, which is a light-demanding species, and probably requires large forest gaps to regenerate (Kitajima & Hogan 2003). We expected rates of adult recruitment and realized population growth to track variation in the gap disturbance regime. Although secondary forests typically lack large numbers of light-gap disturbances, we used airborne waveform LiDAR observations to establish that our results were related to variation in the frequency of canopy disturbance (Drake *et al.* 2003). Data from LiDAR were used to calculate the proportion of sites with canopy height < 10 m throughout the BCI forest. This is approximately 20 m below the mean height of adult *T. guayacan* from field studies on BCI (Fig. 2.7), and is a quantitative index of the frequency of canopy disturbance. Large disturbances were twice as common in old-growth (0.21%) as in secondary forest on BCI (0.12%). Thus, patterns in adult population dynamics are consistent with the hypothesis that gap-dependent adult recruitment is mediating population growth. Because adult abundance increased in relatively low-density old-growth forest, but was closer to replacement in second-growth, our findings suggest that relatively high abundance throughout second-growth forest on BCI probably reflects historical colonization at the time of abandonment of agricultural land on the island.

Annual recruitment was greater during 2004 – 2006 than during 2006 – 2007 (Table 4). Variation in recruitment of this magnitude could be expected in juvenile trees (Chesson &

Warner 1981; Wright *et al.* 2005) but to our knowledge no such spatially extensive recruitment among adult canopy trees has been documented. A recent analysis showed that increases in the frequency of floral and fruit production for trees and lianas on BCI were associated with El Niño Southern Oscillation conditions (Wright & Calderon 2006). In addition to operating directly on the floral production of adult individuals, regional conditions may induce recruitment to the adult life stage for *T. guayacan*. Changing rates of adult recruitment may be partly responsible for long-term trends in flower production observed on BCI, at least for some species. One mechanism that supports this speculation is increasing solar irradiance and relief of light limitation (Saleska *et al.* 2007; Zimmerman *et al.* 2007). It has also been proposed to explain inter-annual variation in reproductive phenology (Wright & Calderon 2006), and rates of canopy photosynthesis throughout the Brazilian Amazon (Saleska *et al.* 2007).

Conclusion

The landscape perspective of canopy tree populations that is possible using remote observations should provide novel insights and better statistical power to test hypotheses about the drivers of population and community dynamics. Although the spectral characteristics of flowering *T. guayacan* were useful in the remote identification of this species, the analytical approach developed here is general and will allow demographic analyses of other canopy tree species using satellite or airborne remote sensing. Widespread monitoring for model species is achievable using contemporary satellite observations. Studies should establish which canopy tree species can be reliably sampled by satellite by focusing on periods of spectral distinctness associated with phenological change (Frankie 1974). Larger numbers of species can be monitored using airborne hyperspectral observations, even in the absence of conspicuous

phenology (Asner & Vitousek 2005; Clark *et al.* 2005; Castro-Esau *et al.* 2006; Carlson *et al.* 2007). Robust statistical tools, coupled with observational platforms that can distinguish greater numbers of species and obtain information on physiological condition (Asner *et al.* 2007), will generate new opportunities in basic and applied research, including causes and consequences of ongoing global change for forest tree populations.

Materials and methods

Study site

We studied the dynamics of adult *T. guayacan* in 15.4 km^2 of tropical moist forest on Barro Colorado Island, Panama using four satellite observations between 2002 and 2007 (Fig 4). BCI is a mosaic of old-growth and second-growth forest (Foster & Brokaw 1996), and is the site of a 50 ha forest dynamics plot in which all free standing woody plants ≥ 1.0 cm DBH have been identified, mapped, and monitored regularly since 1982 (Fig. 2.2). The site receives approximately 2500 mm of rainfall annually, and has a strong dry season from December to April. Mean canopy height is 32.9 m ± 6.4 m S.D. in old-growth forest, and 30.1 m ± 6.2 S. D. in second-growth (Fig. 2.5).

Satellite observations

The QuickBird and Ikonos sensors acquire measurements in four spectral bands over the visible and near-infrared regions of the electromagnetic spectrum at up to 2.44 and 4.0 m spatial resolution, respectively. Image data were acquired on four occasions over 5 years (Table 1). Acquisition at each occasion was timed to coincide with the synchronous annual flowering of adult *T. guayacan* after early wet-season rains. Image data were corrected to apparent surface reflectance using the MODTRAN4 radiative transfer model, implemented using the FLAASH

module of ENVI version 4.3 (ITT Industries Inc.). Preliminary georeferencing was applied at the time of acquisition, and we corrected small distortions using non-linear rubbersheeting, with the most cloud-free (2004) image as a reference (Table 1).

Spectral mixture analysis

We used multiple endmember spectral mixture analysis (MESMA) to map the distribution and abundance of adult *T. guayacan* throughout the BCI forest. MESMA is conceptually similar to traditional SMA, except that it allows the number of endmembers to vary between pixels, and chooses from a set of candidate endmember spectra by minimizing residual variation (Roberts *et al.* 1998; Dennison & Roberts 2003). The model is

$$\rho_{i\lambda} = \sum_{k=1}^{N} f_{ki} \times \rho_{k\lambda} + e_{i\lambda}, \qquad [1]$$

where $\rho_{i\lambda}$ is the observed reflectance for pixel i within multispectral band λ, f_{ki} is the fractional abundance of endmember k within pixel i, $\rho_{k\lambda}$ is the endmember reflectance at band λ, and $e_{i\lambda}$ is a residual term. In practice, $\rho_{k\lambda}$ are estimated from laboratory or image sources, and a constraint is imposed on the model so that

$$\sum_{k=1}^{N} f_{ki} = 1. \qquad [2]$$

We collected endmembers from each image using a pixel purity index by iteratively projecting pixel values onto a randomly oriented vector in multispectral space (Boardman *et al.* 1995).

Pixels that are repeatedly identified as extreme are spectrally pure endmembers. We implemented the PPI for each image using 10,000 iterations, and manually classified extreme pixels into one of four classes: photosynthetic vegetation, cloud, *T. guayacan* floral tissue, or *Jacaranda copaia* (Bignoniaceae) floral tissue. *J. copaia* is a rain forest canopy tree that produces flowers of a blue-purple hue (Fig. 2.1). For images acquired when *J. copaia* adults were flowering, failure to include a *J. copaia* floral endmember would produce errors of commission for *T. guayacan*. This set of candidate endmembers was reduced to 2 – 4 endmembers for each class using standard methods (Dennison & Roberts 2003). The reduced set of image endmembers was used to model the spectrum of each pixel using a combination of two, three, or four endmember models. The best model for each pixel was identified as the model producing the lowest root mean squared error (Roberts *et al.* 1998; Dennison & Roberts 2003).

Due to changes in canopy phenology and cloud cover between image samples, we used endmembers for *T. guayacan*, *J. copaia*, photosynthetic vegetation, and photometric shade (zero reflectance in all bands) in 2002, 2004 and 2007. Patchy cloud cover could not be completely masked from the 2006 image, and *J. copaia* was not flowering at the time of image acquisition. For 2006, we used endmembers for *T. guayacan*, cloud, photosynthetic vegetation, and photometric shade.

Image segmentation

SMA fractional images indicate whether a given pixel is likely to be within a flowering *T. guayacan* crown. However, demographic analyses require mapping individual trees, each of

which may contain one to many image pixels (Fig. 2.1). Segmentation is the process of organizing image data into contiguous thematic objects. We designed a simple algorithm to segment individual rain forest canopy trees for demographic inventory and analysis. The algorithm is implemented in three steps for each image sample. First, the most extreme pixel observation ≥ an estimated threshold is identified within the *T. guayacan* endmember image produced by SMA. Next, values of cardinal neighbors are evaluated. If they are ≥ a stopping threshold, and therefore likely to occur within a flowering *T. guayacan* crown, they are merged with the single-pixel object. Evaluation of neighbors continues until all neighboring pixels are < the stopping threshold. Finally, this procedure is repeated until no pixels ≥ the entry threshold remain unassigned to an object in the endmember image.

Determining the value of the entry threshold is important, because it dictates whether a particular tree will be included in the sample (analogous to a stem diameter threshold in ground-based surveys). Although a complete census is not necessary, if the threshold were too high, sampling would be unnecessarily restrictive. A threshold that is too low will produce errors of commission.

We used logistic regression to determine values of entry thresholds to be applied to each image during segmentation (Table 3). Logistic regression models a binary response (presence or absence of *T. guayacan*) as a function of continuous covariates (*T. guayacan* endmember value). The entry threshold for each image is the endmember value associated with probability of 0.5. To fit logistic regression models and estimate entry thresholds, we randomly sampled 100 pixels with the constraint that ten pixels were required from each bin of 0.1 endmember units (i.e. ten

pixels from 0 – 0.1, ten pixels from > 0.1 – 0.2 etc.). Some bins did not contain 10 pixels, because very high endmember values are uncommon, in which case all pixels within the given bin were included in the sample. Each pixel was visually classified as *T. guayacan* floral tissue [1] or not [0] based on apparent presence or absence of flowering *T. guayacan* using a geographic information system (GIS). Stopping thresholds were determined empirically by examining endmember image values near the edges of flowering *T. guayacan* crowns (Fig. 2.1). Presence of clouds in each satellite image censored some individuals from detection, and produced shadows on the forest canopy (Table 1). Because shadowed areas have reduced brightness, thresholds identified for illuminated canopies are not appropriate. In regions of cloud shadow, we normalized each fractional image pixel by the sum of the non-shade endmember images for that pixel (Adams *et al.* 1993; Powell *et al.* 2007). In shaded areas, we applied the segmentation algorithm to the shade-normalized endmember image.

Upon completion of image segmentation for the entire image time series, we overlaid image segments in a GIS to generate an encounter history for each individual. An encounter history is a series of zeros and ones that indicates whether an individual was observed or not at each sampling occasion. For example, encounter history 1100 is a tree that was observed for the first time in 2002, observed in 2004, and not observed after 2004. We excluded segments along the shore of the island that clearly did not belong to adult *T. guayacan*, and segments caused by poor image quality in deeply shaded areas (i.e. where shade normalizing produced spurious bright values).

Remote estimation of demographic rates

We analyzed encounter histories generated using satellite observations for adult *T. guayacan* in a Bayesian state-space framework to estimate survival, recruitment, and realized population growth (Royle 2008). State-space modeling decomposes observations into two independent components. One component models the underlying but latent demographic process (survival or recruitment). A second component models the observations, conditional on the demographic process (Royle 2008). Let z[i, t] be a vector of Bernoulli random variables that indicates whether individual *i* was alive (1) or not (0) at time *t*. On the first occasion that an individual is observed, *f*, it is assumed to be alive with probability 1. Subsequent states are predicted as independent Bernoulli trials with time-specific probabilities of survival. That is, z[i, t] | z[i, t – 1] ~ Bernoulli($\phi_t \times$ z[i, t – 1]) for all *t* from $f + 1$ to *s*, where *s* is the total number of sampling occasions. Thus, if an individual is alive at $t - 1$, it remains in the living state with time-specific probability of survival, ϕ_t. If it is dead at $t - 1$, it remains dead with probability 1.

The observational process is modeled as independent Bernoulli outcomes conditional on the demographic process. Let x[i, t] be a vector of Bernoulli random variables that describe whether individual *i* was observed (1) or not (0) at time *t*, conditional on the true state: x[i, t] ~ Bernoulli($p_t \times$ z[i, t]). That is, if the individual is alive at *t*, it is observed with probability p_t. If it is dead, it is not observed with probability 1. This state-space formulation is equivalent to the Cormack-Jolly-Seber capture-mark-recapture model that has been used for decades in animal ecology (Cormack 1964; Jolly 1965; Seber 1965; Royle 2008).

Recruitment estimates are made by analyzing observations in reverse time. This approach is mathematically identical to the formulation above, except that conditioning is applied to the last observation *l*, instead of the first, *f*, and the interpretation of state transitions no longer applies to the survival process. Let g[i, t] be a vector of Bernoulli outcomes that indicate whether individual *i* was a member of the adult population at time *t*. In the reverse-time analysis, γ_{t+1} is the seniority probability, which is the likelihood that an adult at $t + 1$ was also an adult at *t*. Because adults at $t + 1$ that were not adults at *t* must have recruited, $1 - \gamma_{t+1}$ is the probability of adult recruitment (Pradel 1996). On the last occasion that an individual is observed, *l*, it is assumed to be an adult with probability 1. Previous states are predicted using time-specific probabilities of seniority. That is, $g[i, t] \mid g[i, t + 1] \sim \text{Bernoulli}(\gamma_{t+1} \times g[i, t + 1])$ for all *t* from *l* - 1 to 1.

In the recruitment analysis, observations are again modeled as independent Bernoulli outcomes conditional on the demographic process. Let h[i, t] be a vector of Bernoulli random variables that describe whether individual *i* was observed (1) or not (0) at time *t*, conditional on the true state: $h[i, t] \sim \text{Bernoulli}(p_t \times g[i, t])$. That is, if the individual is a member of the adult population at *t*, it is observed with probability p_t. If it is not yet recruited, it is not observed with probability 1. This is equivalent to the reverse-time approach to recruitment estimation originally developed by Pradel (Pradel 1996). Over all possible encounters, ϕ_t, p_t, and γ_{t+1} characterize the demographic and sampling process that generates observations of individual trees using remotely sensed data (Table 2).

In practice, the state-space formulations condition on the first detection in the forward-time analysis, and the last detection in the reverse-time analysis. Individuals observed for the first time at the last sampling occasion (2007) therefore cannot contribute information on survival. In the recruitment analysis, individuals observed for the first time on the first occasion (2002), and never observed again, contain no information on recruitment. Thus, sample sizes in the survival and recruitment analyses are not equivalent, and estimated probabilities of detection will correspondingly differ. Out of the 690 trees observed in our study, 6 were observed for the first time in 2007, and 149 were observed in 2002 and never observed again. Therefore, survival estimates are from 1080 observations for 684 individuals, and recruitment estimates are from 937 observations for 541 individuals.

Derivation of the realized population growth rate

With estimates of survival and recruitment, it is straightforward to derive the realized population growth rate (Pradel 1996). Consider a population of N individuals at time t. At the following occasion, t + 1, the size of the population is

$$N_{t+1} = N_t \phi_t + R \qquad [3]$$

where R is the number of individuals that recruited between t and t + 1, and were therefore not members of the adult population at t. By definition, R / N_{t+1} is the probability of recruitment; its complement, $1 - R / N_{t+1}$ is estimated by γ_{t+1},

$$\gamma_{t+1} = 1 - \frac{R}{N_{t+1}}. \qquad [4]$$

Rearranging equation [3] to solve for R and substituting into [4] yields,

$$\gamma_{t+1} = 1 - \frac{N_{t+1} - N_t \phi_t}{N_{t+1}}, \qquad [5]$$

which simplifies to,

$$\frac{\gamma_{t+1}}{\phi_t} = \frac{N_t}{N_{t+1}}. \qquad [6]$$

The right–hand side of [6] is equal to 1 / λ. Therefore,

$$\lambda = \frac{\phi_t}{\gamma_{t+1}} \qquad [7]$$

Thus, remote observations of rain forest canopy trees provide a convenient framework for estimating the essential components of population dynamics, even when detection is imperfect.

Parameter estimation

We obtained parameter estimates from Markov-chain Monte Carlo simulations using Metropolis-Hastings sampling (Lunn *et al.* 2000). The first 10,000 samples were discarded as burn-in, and 10,000 subsequent samples were retained by storing every 20th iteration from each of three Markov chains that were independently initialized. Convergence was assessed using the Gelman-Rubin statistic (Gelman & Rubin 1992), which produces values of 1 if sampling from the target posterior density has been achieved . For all parameters in our analysis, Gelman-Rubin statistics were equal to 1.00.

We specified uninformative prior distributions for all parameters. Survival, detection, and seniority probabilities were drawn from Uniform (0, 1) priors. Additive effects of land use and

individual heterogeneity were Normal (0, σ), where σ was drawn from a Uniform (0, 30) and Uniform (0, 10) in the case of land use and heterogeneity respectively. This approach follows the recommendation of Gelman (Gelman 2006) in the assignment of priors to standard deviation parameters in hierarchical models.

Missing observations

A general framework for remote estimation of demographic rates in rain forest canopy trees must be able to formally deal with missing observations. Persistent cloud cover ensures that some individuals will be censored from observation on each sampling occasion (see supporting information). It is straightforward to incorporate missing observations into a Bayesian analysis. We predicted the unknown observed states for censored individuals by imputing observations using McMC simulation. We are assuming that the observable and unobservable components of our data are generated by the same underlying process, and that censored individuals are unbiased with respect to demographic rates.

Model specification

A priori, we expect survival probabilities to vary minimally through time, and between areas of historical land use on BCI, whereas in the recruitment analysis, we anticipate greater potential for unmeasured variation to influence demographic rates. Although adult recruitment in forest trees is poorly understood, *T. guayacan* probably recruits to the canopy and adult life stage when access to light resources is sufficient (Kitajima & Hogan 2003). This should produce variation in adult recruitment to the extent that heterogeneity in access to light resources exists throughout

BCI. We expect such heterogeneity to be structured by canopy height variability that occurs between areas of historical land use.

Detection probabilities are mediated directly by the expression of carotenoid pigments within flowering canopies, and atmospheric conditions at the time of image acquisition. Indirectly, detection may be influenced by local canopy height, tree size, and access to light resources that dictate reproductive output. Long-term field records indicate that reproductive output varies substantially through time for adult *T. guayacan* (Wright & Calderon 2006). Because it is a light demanding species (Kitajima & Hogan 2003), we expected heterogeneity in detection to occur between individuals associated with unmeasured covariates such as tree height and crown exposure.

We estimated demographic and detection probabilities in the survival and recruitment analysis using hierarchical logit-linear models:

$$\Pr\{z[i, t]\} = \beta_{z,\ \text{time}} + \beta_{z,\ \text{land use}} \quad [M1]$$

$$\Pr\{x[i, t]\} = \beta_{x,\ \text{time}} + \eta_{x,i} \quad [M2]$$

$$\Pr\{g[i, t]\} = \beta_{g,\ \text{time}} + \beta_{g,\ \text{land use}} \quad [M3]$$

$$\Pr\{h[i, t]\} = \beta_{h,\ \text{time}} + \eta_{h,i} \quad [M4]$$

where the response is a binomial probability that predicts the true or observed state for individual *i* at time *t*. The β coefficients describe additive effects of time and land use history on the binomial outcome, and η are random effects that allow probabilities of detection to vary for each individual. Thus, we are allowing survival and recruitment parameters to vary through time and between areas of historical land use. Detection probabilities vary through time, and incorporate individual heterogeneity.

Sample validation

To define the scope of our sample and evaluate potential for bias, we conducted field searches throughout > 28 km of forest during March and April, 2007 (Fig. 2.6). Because this period included the synchronous flowering of adult *T. guayacan*, we opportunistically sampled adult individuals that were in flower. This sample was obtained blindly with respect to satellite observations, and is a benchmark against which to compare individuals detected remotely. We refer to this ground-based sample as the 'ground reference.' We also located trees in the field that had been identified first using satellite observations, using compass orienteering, and maps of adult *T. guayacan* produced by image segmentation. For all trees, stem diameter (cm) was measured at breast height, or above basal irregularities such as buttresses in most cases, to the nearest mm using a diameter tape. Tree height was measured to the nearest m using a hand-held laser range finder. If the sample of trees obtained remotely is representative of adult *T. guayacan*, the ground reference sample and sample of trees identified remotely should contain many of the same individuals, and comparison should not be qualitatively or statistically different.

Acknowledgements

We thank S. Bohlman, D. B. Clark, L. A. Donovan, J. Emmons, W. B. Emmons, J. Lake, D. Lanier, M. Madden, H. Muller-Landau, D. R. Peart, C. Peterson, S. J. Wright, and the Center for Remote Sensing and Mapping Science at The University of Georgia for assistance. We thank C. Colvin, B. McCarty, B. Thomassie, M. Brender, S. Cowen and A. Poole for help with logistics of satellite data collection. This project was funded by a grant from the NSF to S. P. H., and a DDIG to J. R. K.

Fig. 2.1. Demographic inventory using satellite observations. **A**, Flowering adult *Tabebuia guayacan* (left arrows) are conspicuous yellow objects in QuickBird satellite observations from March 21, 2004, for a 14 ha sample of old-growth forest on Barro Colorado Island, Panama. **B**, Spectral mixture analysis predicted fractional abundance of *T. guayacan* floral tissue within every image pixel, and facilitated objective, unbiased sampling of adult trees. Yellow contour intervals at 0.314 are based on logistic regression, and distinguish pixels that are likely to occur within a flowering *T. guayacan* crown. **C**, Fractional images were processed using an automated crown segmentation algorithm to sample individuals throughout a tropical rain forest landscape (red segments). The vertical scale bar is 20 m. Flowering crowns of the rain forest canopy tree *Jacaranda copaia* (right arrows) are also apparent in the upper right portion of the image. The status of one *T. guayacan* is visually ambiguous in this image (upward arrow), demonstrating the necessity of objective sampling criteria. It was detected in 2006.

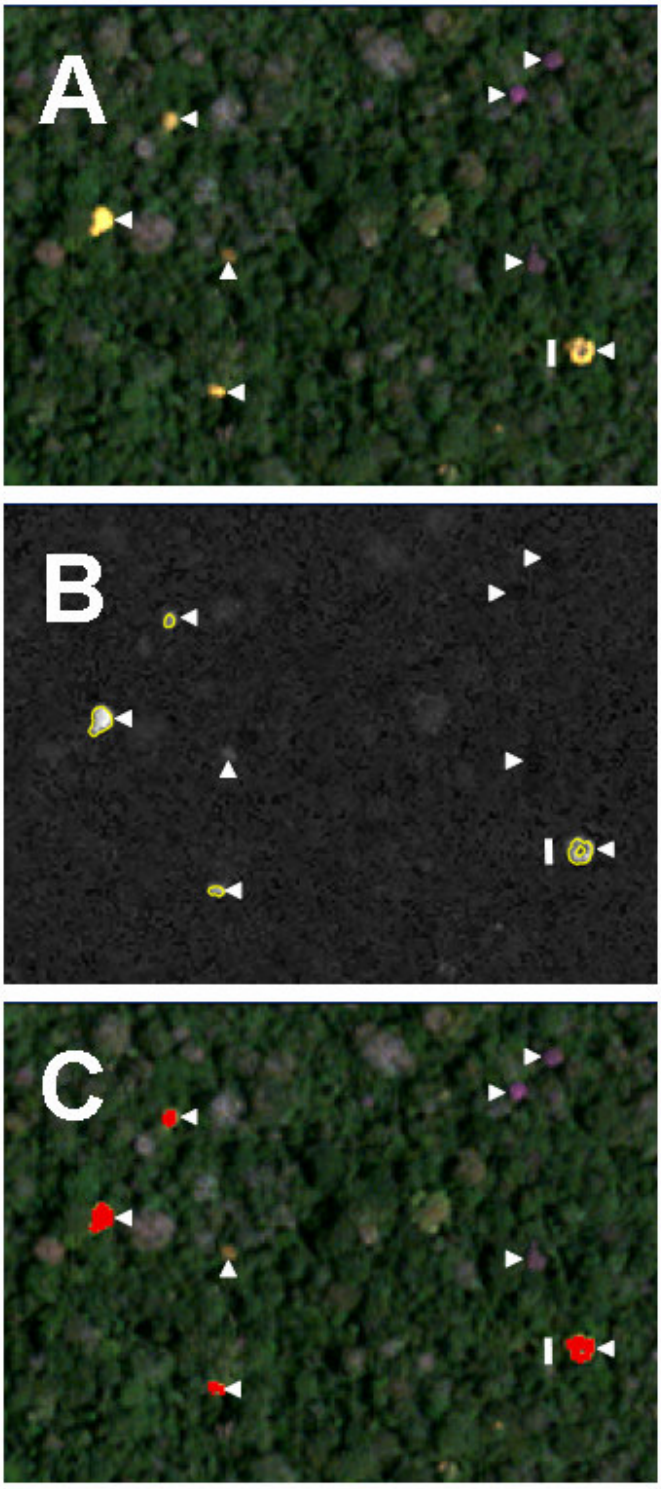
A
B
C

Fig. 2.2. Barro Colorado Island, Panama. Locations of 690 adult canopy trees (*Tabebuia guayacan*) sampled on four occasions during five years using satellite observations. Colors indicate forest classes: dark green (old-growth forest), light green (second-growth forest), white (cut since 1914), yellow (cleared or developed area). The 50-ha forest dynamics plot is shown for scale (1000 × 500 m). The 14-ha box north of the plot depicts the area shown in Fig. 2.1.

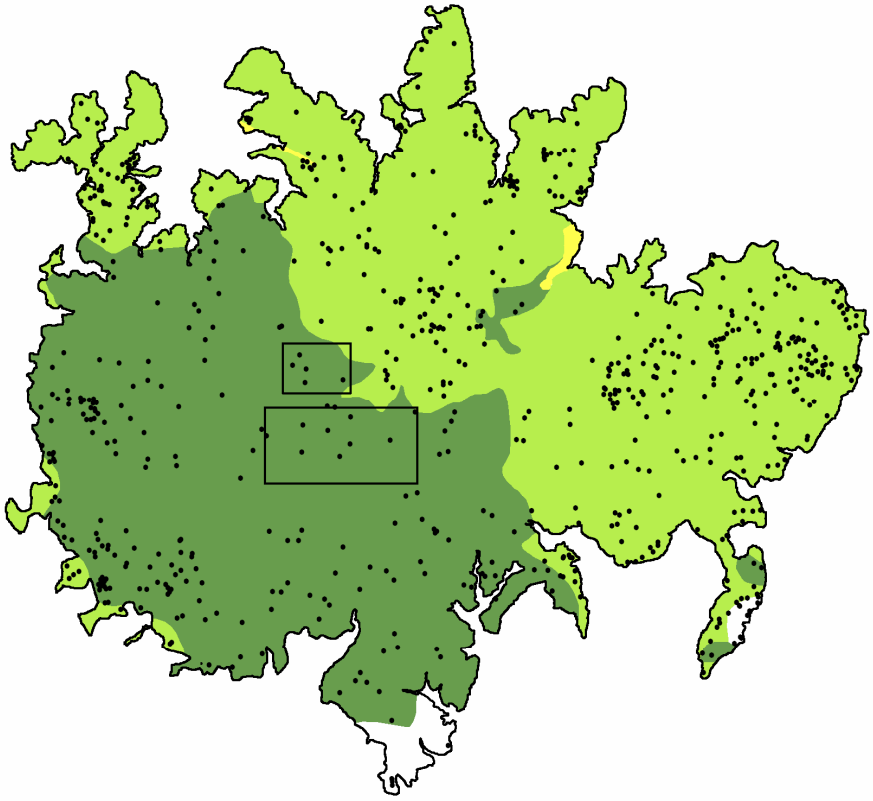

Fig. 2.3. Demographic rates for adult canopy trees. Annualized posterior probability densities for survival, recruitment and realized population growth for adult *Tabebuia guayacan* in old-growth (solid line) and second-growth (dashed line) forest. Estimates are from satellite observations and McMC methods. Dotted vertical line at survival 0.991 is annual survival for *T. guayacan* ≥ 20 cm DBH from an independent field sample. Rates of survival are independent of historical land use, but recruitment and realized population growth were higher in old-growth forest.

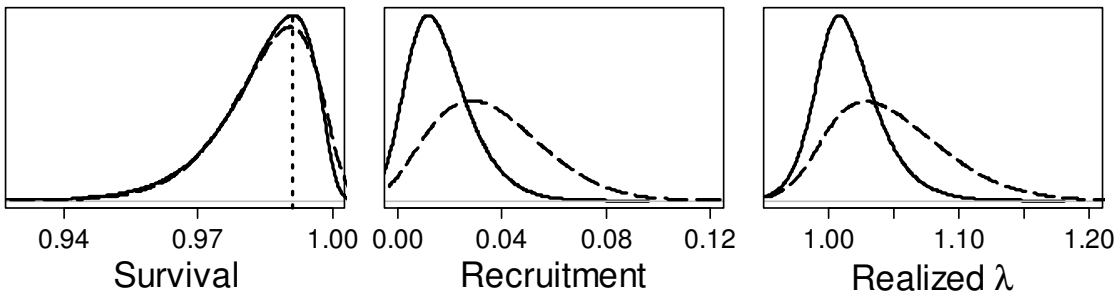
0.94
0.97
1.00
Survival
0.00
0.04
0.08
0.12
Recruitment
1.00
1.10
1.20
Realized λ

Fig. 2.4. Overview of the analytical approach. Demographic inventory and analysis of rain forest canopy trees includes three major components: (i), spectral mixture analysis to identify pixels likely to occur within a flowering *T. guayacan* crown, (ii), image segmentation to generate demographic samples of adult trees, and (iii), modeling observations of individuals through time to estimate demographic rates.

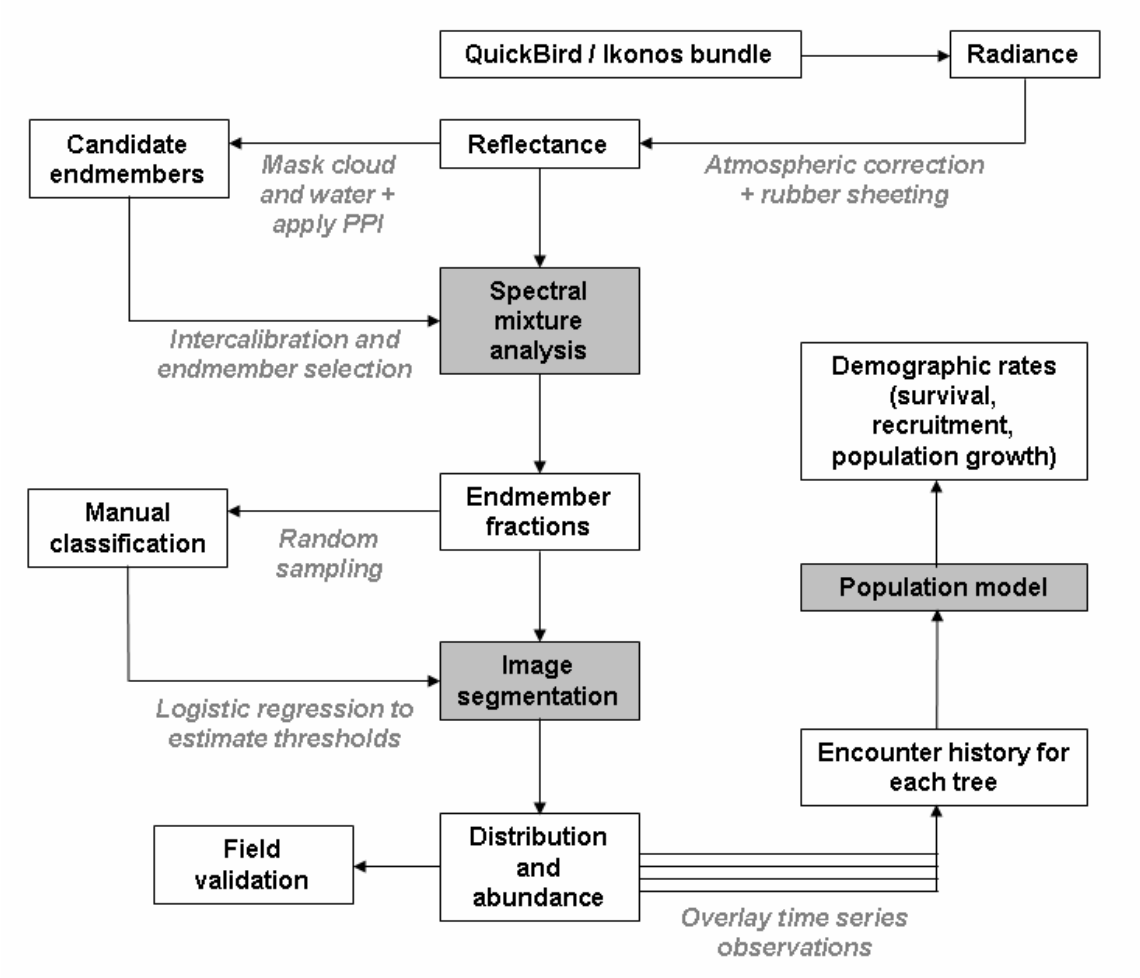
QuickBird / Ikonos bundle
Radiance
Candidate endmembers
Reflectance
Mask cloud and water + apply PPI
Atmospheric correction + rubber sheeting
Spectral mixture analysis
Intercalibration and endmember selection
Demographic rates (survival, recruitment, population growth)
Manual classification
Endmember fractions
Random sampling
Population model
Image segmentation
Logistic regression to estimate thresholds
Encounter history for each tree
Field validation
Distribution and abundance
Overlay time series observations

Fig. 2.5. Canopy height distribution on Barro Colorado Island, Panama. **a**, old-growth forest, **b**, second-growth forest. Mean canopy height is 32.9 m ± 6.43 SD, and 30.1 m ± 6.2 SD, based on n = 47,415, n = 46,076 LiDAR observations respectively.

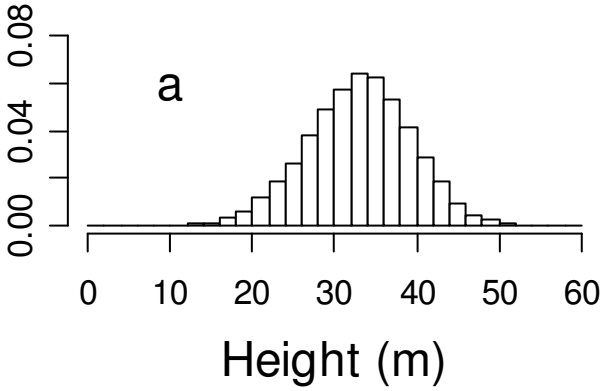
a
0.00
0.04
0.08
0
10
20
30
40
50
60
Height (m)

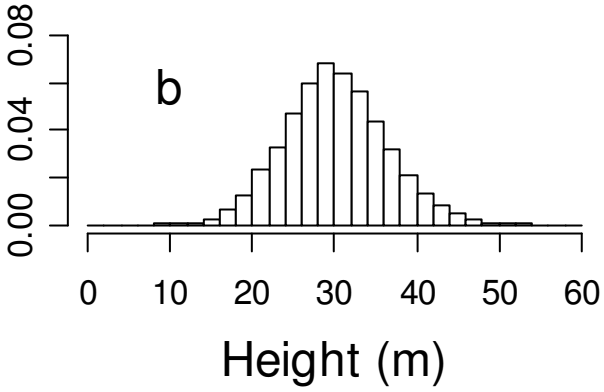
b
0.00
0.04
0.08
0
10
20
30
40
50
60
Height (m)

Fig. 2.6. Location of 167 adult canopy trees (*T. guayacan*) checked in the field on Barro Colorado Island, Panama during March and April, 2007. The samples from satellite observations are unbiased with respect to field data (*P* for stem diameter = 0.576, *P* for height = 0.832). Colors indicate forest classes: dark green (old-growth forest), light green (second-growth forest), white (cut since 1914), yellow (cleared or developed area). The 50-ha forest dynamics plot is shown for scale (1000 × 500 m).

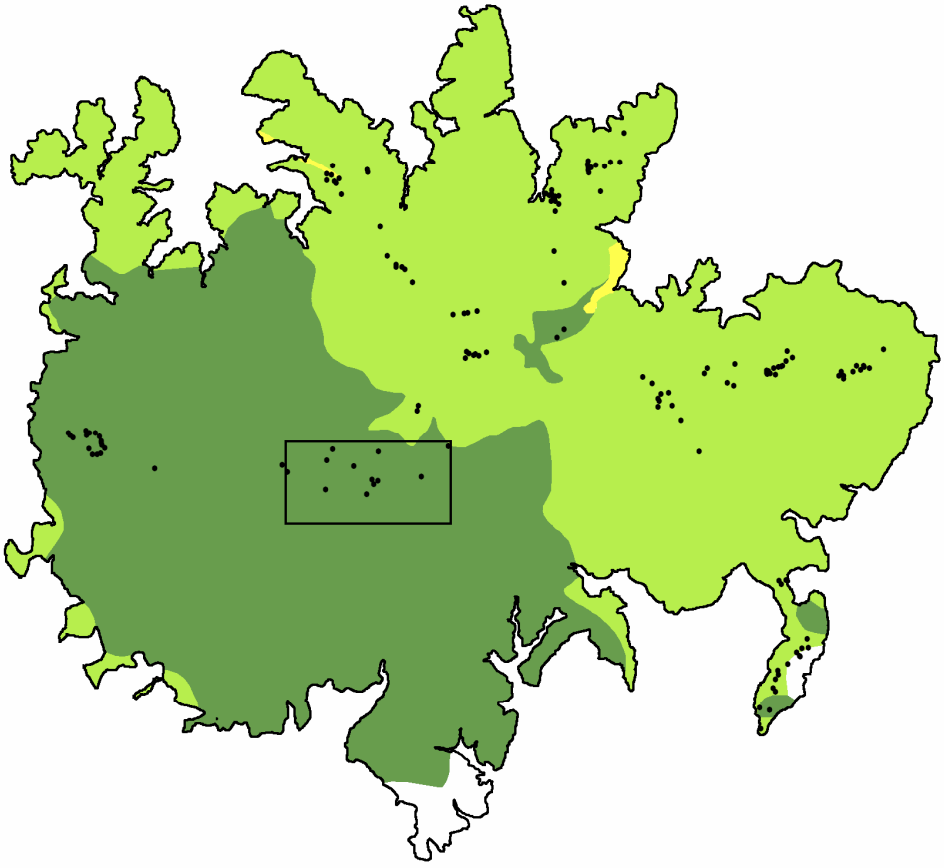

Fig. 2.7. Stem diameter and height distribution for adult canopy trees (*T. guayacan*) on Barro Colorado Island, Panama. **a**, diameter of stems detected by satellite, **b**, height of trees detected by satellite, **c**, diameter of stems from an independent ground reference sample, **d**, height of trees from the ground reference sample. Eighty-two percent of the trees in the ground reference sample were also detected by satellite at least one time. The samples from satellite observations are unbiased with respect to field data (*P* for stem diameter = 0.576, *P* for height = 0.832).

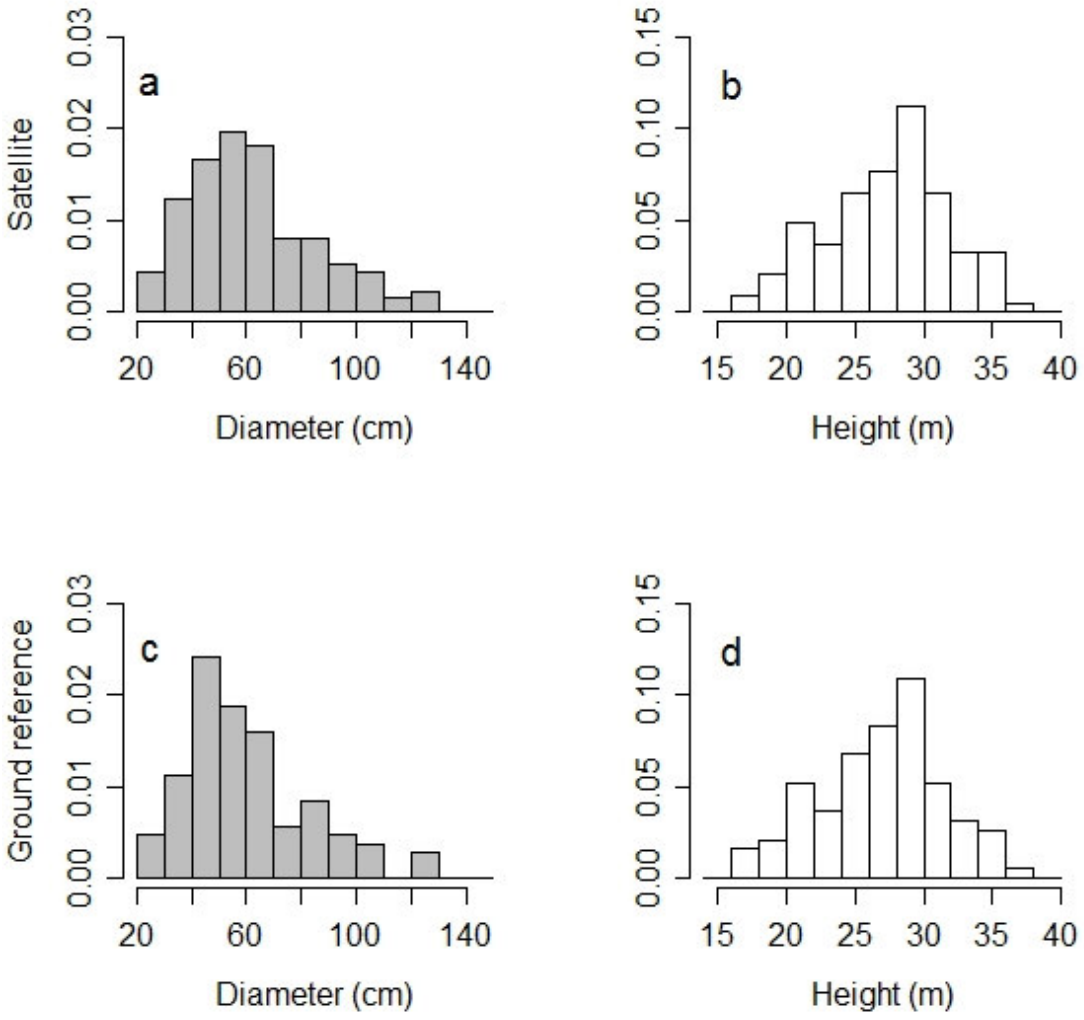
a
b
c
d
Satellite
Ground reference
0.00
0.01
0.02
0.03
0.05
0.10
0.15
20
60
100
140
15
20
25
30
35
40
Diameter (cm)
Height (m)

Table 2.1. Summary of satellite observations for Barro Colorado Island, Panama. Satellite data were acquired on four occasions from the QuickBird and Ikonos sensors. Values are the number of trees detected on each sampling occasion, and the area of the island obscured by cloud cover.

Date	3/29/2002	3/21/2004	4/1/2006	3/20/2007
Satellite	QuickBird	QuickBird	QuickBird	Ikonos
No. trees	380	303	331	75
Cloud (ha)	39.3	7.4	630.4	290.4

Table 2.2. State combinations for individual trees observed using remotely sensed data. A given tree may be observed (1) or not (0) if it is present (P) or absent (A) in the adult population, and detected remotely. True states are dictated by survival and recruitment (left two columns). Inference using observed states alone is not robust, because > 1 true state can produce most observations.

Death	Recruit	TRUE	Obs1	Obs2	Obs3	Obs4	Obs5	Obs6
No	No	PPPP	1111	1110	1101	1011	0111	1100
Yes	No	PPPA	NA	1110	NA	NA	NA	1100
Yes	No	PPAA	NA	NA	NA	NA	NA	1100
Yes	No	PAAA	NA	NA	NA	NA	NA	NA
Yes	Yes	APPA	NA	NA	NA	NA	NA	NA
Yes	Yes	APAA	NA	NA	NA	NA	NA	NA
Yes	Yes	AAPA	NA	NA	NA	NA	NA	NA
No	Yes	APPP	NA	NA	NA	NA	0111	NA
No	Yes	AAPP	NA	NA	NA	NA	NA	NA
No	Yes	AAAP	NA	NA	NA	NA	NA	NA

Table 2 continued

Obs7	Obs8	Obs9	Obs10	Obs11	Obs12	Obs13	Obs14	Obs15
1010	0110	1001	0101	0011	1000	0100	0010	0001
1010	0110	NA	NA	NA	1000	1000	1000	NA
NA	NA	NA	NA	NA	1000	100	NA	NA
NA	NA	NA	NA	NA	1000	NA	NA	NA
NA	0110	NA	NA	NA	NA	0100	0010	NA
NA	NA	NA	NA	NA	NA	0100	NA	NA
NA	NA	NA	NA	NA	NA	NA	0010	NA
NA	0110	NA	0101	0011	NA	0100	0010	0001
NA	NA	NA	NA	0011	NA	NA	0010	0001
NA	NA	NA	NA	NA	NA	NA	NA	0001

Table 2.3. Logistic regression parameter estimates for presence (1) or absence (0) of apparent *T. guayacan* floral tissue. Estimates are from up to 100 randomly selected pixel observations from spectral mixture analysis (SMA) using QuickBird or Ikonos satellite data. Values in parentheses are *P* values testing the hypothesis that the coefficient is equal to zero. P(50) is the SMA value associated with probability 0.5, and was used as a minimum threshold for detection in demographic samples obtained using satellite data. 'Stop' is an empirically defined stopping threshold that was applied to an automated tree-crown segmentation algorithm. Sample size (n) is the number of pixel observations included in the logistic regression.

Date	3/29/2002	3/21/2004	4/1/2006	3/20/2007
Satellite	QuickBird	QuickBird	QuickBird	Ikonos
Intercept	-11.406 (0.008)	-11.825 (0.004)	-8.949 (0.001)	-7.768 (< 0.001)
Slope	42.079 (0.007)	37.627 (0.004)	29.843 (< 0.001)	23.796 (< 0.001)
P(50)	0.271	0.314	0.298	0.326
Stop	0.220	0.220	0.220	0.190
n	100	99	100	81

Table 2.4. Demographic rates for adult *T. guayacan*. Numbers are median estimates from the annualized posterior distribution, with Bayesian credible interval in parentheses. In the survival and recruitment analyses, state transition and detection probabilities over the final interval are not independently estimable (NE). This corresponds to the 2006 – 2007 interval in the survival analysis, and the 2002 – 2004 interval in the recruitment analysis.

	02 – 04 (Annualized)	04 – 06 (Annualized)	06 – 07 (Annualized)	02 – 06 (Annualized)
Survival				
Old	0.985 (0.935 – 0.999)	0.991 (0.959 – 0.999)	Not estimable	0.987 (0.958 –
Second	0.986 (0.939 – 0.999)	0.992 (0.960 – 0.999)	Not estimable	0.987 (0.961 –
Recruit				04 – 07 (Annualized)
Old	Not estimable	0.051 (0.003 – 0.134)	0.020 (0.000 – 0.106)	0.033 (0.005 –
Second	Not estimable	0.022 (0.001 – 0.076)	0.009 (0.000 – 0.048)	0.014 (0.002 –
λ				04 – 06 (Annualized)
Old	Not estimable	1.041 (0.983 – 1.142)	Not estimable	Same
Second	Not estimable	1.012 (0.975 – 1.072)	Not estimable	Same

CHAPTER 3

CANOPY GAPS AND THE DYNAMICS OF A TROPICAL WET FOREST[2]

[2] Kellner, J.R., Clark, D.B. and S.P. Hubbell. To be submitted to *Ecology Letters*.

Abstract

We combined LiDAR remote sensing with field measurements of canopy height to quantify the structure and dynamics of an old-growth Neotropical rain forest in the Atlantic lowlands of Costa Rica. Persistent disturbance figures prominently in the dynamics of this forest. Forty-one percent of the old-growth landscape had net canopy height changes ≥ 5 m during 8.5 years. Most gaps in the forest canopy were small, and individual gap sizes and neighbor distances followed power-laws with slopes that were indistinguishable between years. Gap sizes were unbiased with respect to topographic slope and soil Phosphorus. Despite substantial dynamics, our results demonstrate consistency in characteristics of forest disturbance at large spatial scales, and suggest that changes in canopy height were very close to the steady-state equilibrium expectation. These findings challenge the view that Neotropical forests are undergoing structural degradation in response to global changes, and provide evidence of the necessary conditions for selection for long-distance dispersal.

Introduction

In closed-canopy tropical rain forests, localized canopy openings occur that mediate access to light and space in the forest understory (Brokaw 1982, 1985; Hubbell & Foster 1986b). These 'canopy gaps' are caused by the death of, or damage to, a canopy-forming tree. Quantifying the sizes and spatial properties of gap distributions on landscapes is fundamental to understanding the diversity and evolution of forest tree species (Denslow 1980; Hubbell & Foster 1986b; Hubbell *et al.* 1999). For many species, gaps are essential at some stage in ontogeny for individuals to recruit to the canopy.

There is evidence that gap areas follow power-law size distributions, as most gaps in the forest canopy are small and extremely large gaps are rare (Hubbell & Foster 1986b; Sanford *et al.* 1986; Nelson *et al.* 1994). Work from tropical moist forest on Barro Colorado Island, Panama (BCI) has shown that probabilities of gap occurrence are higher near the edges of existing gaps, and that filling can occur through both upward and lateral growth from adjacent canopy trees (Young & Hubbell 1991). Gaps tend to occur more frequently on slopes than on flat terrain (Clark *et al.* 1996), and may be more abundant on fertile sites. However, sources of variation in gap distributions on landscapes are poorly understood. By *landscapes* we are referring to the areas at which forests are perceived by interacting tree species. For individuals, this area is arguably determined by the density of seed dispersal. Molecular analyses have shown that dispersal is occurring over distances of hundreds of meters, and sometimes much greater (Jones *et al.* 2005; Hardesty *et al.* 2006; Sezen *et al.* 2007). This distance is farther than those sampled within most field inventory plots. Over their evolutionary lifetimes, species perceive forested

landscapes throughout vastly larger areas that are dictated by range sizes. Range sizes for most tropical tree species have not yet been mapped empirically, but are very large, as individuals of the same species can be observed in plots separated by great distances, and species turnover occurs very slowly over thousands of kilometers (Condit 2002; ter Steege 2006; Hubbell *et al.* 2008).

Limitations to observing the structure and dynamics of tropical forest canopies throughout large areas have two main causes. It is difficult to sample ephemeral, rare events, and challenging to consistently define gap versus non-gap areas. Recently-disturbed gap sites represent a small fraction of a forested landscape, typically on the order of a few percent by area (Hubbell & Foster 1986b; Sanford *et al.* 1986). A secondary issue is inconsistent application of minimum-area and maximum-height thresholds for defining gap versus non-gap areas, and difficulty estimating canopy height under demanding field conditions (reviewed in Clark & Clark 1992).

In this study, we combine LiDAR remote sensing with field measurements of canopy height to characterize the size frequency distribution, spatial characteristics, and dynamics of canopy gaps in an old-growth Neotropical rain forest in the Atlantic lowlands of Costa Rica. By recording the return-time of reflected laser pulses, LiDAR sensors acquire physically-based measurements of canopy height and ground elevation (m), and the vertical and horizontal distribution of biomass (Drake *et al.* 2002a; Drake *et al.* 2003; Clark *et al.* 2004c; Asner *et al.* 2008). They are ideal for quantifying the structure and dynamics of forest canopies, because they provide spatially referenced, extensive and finely grained vegetation height measurements that are objectively

acquired. LiDAR measurements facilitate access to characteristics of forest canopies at multiple scales, and permit objective analyses of canopy structure and dynamics on landscapes.

Methods

Site description

This study was conducted in old-growth rain forest at the La Selva Biological Station, in the Atlantic lowlands of Costa Rica (Fig. 3.1). The site is classified as Tropical Wet Forest in the Holdridge life-zone system (Hartshorn & Hammel 1994) and receives approximately 4000 mm of rainfall annually (Sanford *et al.* 1994). Mean monthly temperature is 26° C and relief ranges from 39 to 153 m on highly weathered Oxisols (Kleber *et al.* 2007). Mean canopy height is 20.4 m ± 6.9 m S.D. (this study). The density of stems ≥ 10 cm diameter at breast height (DBH) is 504 ± 22 · ha^{-1} and estimated aboveground biomass is 160.5 ± 4.2 Mg · ha^{-1} (Clark & Clark 2000). Leaf area index (LAI) is 6.00 ± 0.32 (S.E.), and increases linearly with canopy height up to 21 m (Clark *et al.* 2008). Most of the study site is on undulating upland plateaus for which there is no evidence of extensive historical human land use (Kennedy & Horn 2008).

Light Detection and Ranging

We used data collected 8.5 years apart from two LiDAR systems to quantify canopy height changes. The FLI-MAP system and Leica ALS50 are discrete pulse, scanning laser altimeters. Data from the FLI-MAP sensor were acquired for 445 ha of old-growth rain forest on September 12 – 13, 1997 (John E. Chance and Associates, Lafayette, Louisiana, USA, Fig. 3.1). Scan angle was 33 º, and beam divergence 2 milliradians. The data were collected by helicopter from 70 m

aboveground, producing 0.14 m pulse diameters at ground elevation, and were provided as a 0.33 m raster digital surface model (DSM) that had been generated by the data provider using proprietary methods. Each 0.33 m DSM pixel contained a single elevation value in meters (ground elevation + vegetation height). Clark et al. (2004c) identified pixels that were likely to represent ground elevation within the DSM (i.e. where vegetation height = 0) and interpolated a 1 m raster ground surface (digital terrain model, DTM). Subtraction of the DTM from the DSM produced a 0.33 m raster of canopy height above ground (digital canopy model, DCM, Fig. 3.2). Comparison of vegetation height and ground elevation from field and FLI-MAP sources indicates that relationships are precise and accurate when tree height can be measured reliably in the field (Clark *et al.* 2004c).

The Leica ALS50 collected LiDAR observations for 64 km^2 of tropical wet forest on March 13 – 14 2006. Beam divergence was 33 milliradians, which produced 0.33 m pulse diameters at ground elevation from the 1000 m collection altitude aboard a fixed-wing aircraft (Cognocarta GIS LLC, San Jose, Costa Rica). Mean sampling density was 1 pulse $\cdot$ m^{-2} in old-growth forest. The complete data set is publicly available (Kellner *et al.* unpublished manuscript), and contains 115,058,607 LiDAR measurements for the La Selva property and lower flanks of Parque Nacional Braulio Carillo, spanning gradients in mixed agro-natural land use and soil fertility. We focus here on the 445 ha of old-growth forest for which data were collected by the Leica ALS50 and the FLI-MAP system (Fig. 3.1).

Height models and canopy dynamics

We processed the FLI-MAP DSM and point elevation estimates from the Leica ALS50 to generate 5 m DSMs. Each 5 m pixel contains the mean of all elevation measurements within the given pixel. For data from the FLI-MAP system, most 5 m pixels contained 225 pixels of 0.33 m. Elevation estimates for some 5 m pixels were based on smaller samples, because we excluded areas that were near edges or between flight lines, for which no LiDAR data were collected. For the data from the Leica ALS50, the sample size for each 5 m pixel was the number of LiDAR pulse observations within the given pixel, which ranged from 1 to 94, with mean and standard deviation equal to 25.9 and 7.9 respectively.

To estimate canopy height above ground, we generated 5 m DTMs from FLI-MAP and Leica ALS50 data, and subtracted the respective DTM elevation from DSMs to produce digital canopy models. For the FLI-MAP system, we resampled the 1 m DTM generated by Clark et al. (2004c) to 5 m using nearest-neighbor resampling. For the Leica ALS50 we generated a 5 m DTM by applying a natural neighbor interpolation to point elevation estimates that were classified as ground elevation by the data provider using proprietary methods (Cognocarta GIS LLC, San Jose, Costa Rica). Based on a data set of 4184 ground-surveyed control points, the relationship between field and Leica ALS50 LiDAR estimates of ground elevation is accurate throughout the range of topographic and structural conditions within old-growth forest at La Selva: field measured elevation (m) = 0.999 × LiDAR predicted elevation (m) – 0.423 m, $P < 0.001$, $r^2 =$ 0.994, RMSE = 1.84 m (Kellner *et al.* unpublished manuscript).

To examine changes in canopy height between 1997 and 2006, we first coregistered the 2006 Leica DSM to the 1997 FLI-MAP DSM using a geographic information system to correct a small offset between data sources. The correction was an affine transformation applied to six control points that were well-distributed throughout the old-growth study area. Overall RMSE was 1.24 m, which is smaller than side length of a single DSM pixel. We then subtracted the 1997 FLI-MAP DSM from the 2006 Leica ALS50 DSM to produce a model of canopy height change.

Each height-change pixel contained a single value that was the net change in canopy height (m) between 1997 and 2006, where positive values indicated height gain, and negative values indicated height loss. Although subtraction of canopy height or elevation estimates should produce equivalent results, in practice changes calculated using DCMs incorporate errors associated with estimation of ground elevation. We therefore calculated height changes using canopy elevation to avoid propagating these errors into the estimates of canopy height change. We assumed that DSMs are accurate, and that ground elevation has not changed significantly between the LiDAR surveys, so that differences between DSMs characterize vegetation dynamics, rather than changes to underlying topography or LiDAR error. This assumption is likely to be correct, given that old-growth forest at La Selva is on stable terrain, DTM estimates throughout the old-growth landscape from 1997 and 2006 are highly correlated ($r = 0.997$), and LiDAR elevation measurements can be proven highly precise and accurate when high-quality validation data are available. Indeed, a major challenge in demonstrating the accuracy of LiDAR measurements is obtaining sufficiently better data for validation.

Gap definition

We quantified the size frequency distribution of gaps in the forest canopy by applying Brokaw's definition to the 5 m DCMs. A gap is "a 'hole' in the forest extending through all levels down to an average height of two m above ground" (Brokaw 1982). LiDAR remote sensing is ideal for distinguishing gap versus non-gap areas, because it minimizes the potential for subjective assessments to influence conclusions (see discussion in Clark & Clark 1992), and allows gap definitions to be applied consistently throughout large areas. The smallest gap observable in this study was a single 5 m × 5 m pixel of 25 m^2, and any of the eight neighbors with vegetation height ≤ 2 m were part of the same Brokaw gap (i.e. if three pixels shared at least one side or corner and had vegetation height ≤ 2 m, they were classified as a single Brokaw gap that was 75 m^2 in area).

Height transitions

We quantified canopy height transitions by examining properties of the transition matrix, **A**, for 1 m height classes between 0 and 40 m throughout old-growth forest at La Selva. The **A** matrix integrates growth and lateral filling, mortality and branch loss that characterize canopy dynamics. It is similar to a Lefkovitch population projection matrix, except that transition probabilities apply to height changes at a given location rather than survival and reproduction, and the first row of the matrix does not contain fertilities. Instead, element $\mathbf{A}_{[i,j]}$ contains the probability that the height class at column *j* will enter the height class at row *i* during the 8.5 year transition interval. Thus, rows one and two contain the probabilities that column *j* will produce a gap < 2 m in height, and the **A** matrix contains 1,600 empirically estimated transition probabilities. We calculated the steady-state distribution of canopy height by solving for the

dominant eigenvector of the height transition matrix (Caswell 2000). A subset of the **A** matrix is in Table 3.1, and the full transition matrix is in Appendix A.

Structure and dynamics

We examined spatial properties of the distribution of Brokaw gaps by quantifying the mean distance to the *n*th nearest neighbor gap for all gaps in 1997 and 2006. To test whether there was clumping or overdispersion, we randomized the locations of all *n* gaps in 1997 and 2006 within the old-growth study area, and recalculated the mean distance to the *n*th nearest neighbor gap. This procedure was repeated 1,000 times to predict the expected value under the null hypothesis of complete spatial randomness.

Independent of patterns of occurrence in gap locations, gap sizes could also show non-random spatial distributions. For example, stem density at La Selva is highest on slopes, and lowest on alluvial terraces (Clark & Clark 2000). Gradients in soil fertility at La Selva are influenced by substrate aging and erosion. Although most of the landscape is low in soil P, Porder *et al*. (2006) demonstrated using Strontium isotopes that the fraction of rock-derived nutrients increases on slopes, suggesting that erosion rejuvenates nutrient supply on deeply weathered soils at La Selva. Espeleta & Clark (2007) showed that plant investment in fine root biomass was higher in low-fertility upland plateaus than in relatively fertile alluvial terraces. We therefore expected elevated rates of canopy turnover and smaller gaps to occur in the most fertile sites, where nutrient limitation could be reduced, and on slopes where stem density is higher. We tested this prediction by examining correlation coefficients between gap size and topographic slope or predicted soil P. Slope was calculated in degrees using the 5 m Leica DTM. Soil P was

predicted on a 30 m × 30 m raster throughout old-growth forest using ordinary kriging. Predictions were based on 2123 field measurements of soil P that were collected on a 50 × 100 m sampling grid (J. Powers, unpublished manuscript).

Field measurements

Our conclusions depend on the ability of LiDAR height measurements to quantify forest structure and dynamics. We obtained field measurements of canopy height within 18 0.5 ha plots (the CARBONO project, Clark & Clark 2000, Fig. 3.1). Each plot is 100 × 50 m, and was randomly sited within old-growth forest at La Selva and stratified by dominant topographic and fertility gradients (Clark & Clark 2000). Within each plot, all stems ≥ 10 cm diameter at breast height or above irregularities such as buttresses (DBH) have been identified, mapped and monitored annually since 1998. Measurements of vegetation height between 1.50 m and 15.00 m were made on a 5 m × 5 m sampling grid within each plot to the nearest cm using a Hastings measuring pole between June and August 2006. Thus, we compared field measurements of canopy height to LiDAR data from the Leica ALS50, but not the FLI-MAP system, for which we rely on the validation of Clark *et al*. (2004c). At each site, the height measurement was the maximum vegetation height directly above the point of measurement on the 5 m sampling grid. Because of the difficulty of precisely establishing which branch or leaf is directly over a given point of measurement, field technicians visualized a 2 m × 2 m quadrat projected upward to the canopy using a hand-held clinometer. Holes in the forest canopy that were smaller than 2 m × 2 m were treated as closed canopy. Sites with vegetation height outside the measurable range were given discrete classifications (i.e. '< 1.50 m' or '> 15.00 m'). There were 231 height

measurements made in the field within each 0.5 ha plot, and a total of 4158 vegetation height measurements were compared to LiDAR data.

To compare the size frequency distributions of Brokaw gaps identified using field and LiDAR data, we identified gaps in the forest canopy within each plot using the same criteria used for the LiDAR data. Each site on the 5 m × 5 m field sampling grid was classified as 'gap' or 'non-gap' based on the point estimate of vegetation height. Sites with field measured vegetation height < 2 m were in Brokaw gaps, and adjacent gap sites were part of the same gap object.

We anticipated that the largest forest gaps might not be represented using field-based sampling (Fearnside 2000; Clark 2004). Such an outcome is expected based on the smaller area sampled in plots (9 ha) compared to the landscape (445 ha), but could also occur if there is systematic bias between field and LiDAR data. To determine whether the size frequency distributions of Brokaw gaps are similar between field and LiDAR sources, we used bootstrap simulations. Each simulation selected a random sample of *n* Brokaw gaps from the larger number observed using LiDAR in 2006, and calculated the size frequency distribution, where *n* is the number of Brokaw gaps identified within plots using field methods. This process was repeated 1,000 times to generate confidence intervals for the expected size frequency distribution under the null hypothesis of no systematic difference between field and LiDAR data. This analysis allowed us to test the hypothesis that the absence of the largest gaps within plots is a sampling artifact.

Results

Canopy dynamics

Old-growth forest at La Selva was dynamic (Fig. 3.3, Table 3.1). Forty-one percent (182 ha) of the old-growth landscape had net height changes ≥ 5 m. Low canopy sites were likely to increase in height during our 8.5-year study, and most sites in the upper canopy had height loss: change in canopy height (m) = 10.13 – 0.51 × canopy height in 1997, $P_{\text{intercept}} < 0.001$ $P_{\text{slope}} < 0.001$, $r^2 = 0.281$, RMSE = 5.96, n = 177,855 (Fig. 3.4). The dominant eigenvector from the height transition matrix indicates that the distribution of canopy height was close to the steady-state expectation in 1997 and 2006 (Fig. 3.5). Although substantial dynamics occurred during the 8.5 year study (Figs. 3.3, 3.4), the distribution of canopy height remained similar between years (Fig. 3.5).

Canopy gap locations and sizes

Sizes and neighbor distances of canopy gaps followed power laws (Fig. 3.6). In both 1997 and 2006, the expected number of gaps of a given size decreased linearly on a log-log plot: frequency in 1997 = 5.45 – 2.26 × gap area (m^2), $P_{\text{intercept}} < 0.001$ $P_{\text{slope}} < 0.001$, $r^2 = 0.914$, RMSE = 0.23, n = 9; frequency in 2006 = 5.51 – 2.36 × gap area (m^2), $P_{\text{intercept}} < 0.001$ $P_{\text{slope}} < 0.001$, $r^2 = 0.979$, RMSE = 0.112, n = 8. The expected distance to the *n*th nearest gap increased as a power-law function of rank *n* in both 1997 and 2006: distance in 1997 (m) = 1.58 + 0.72 × neighbor rank, $P_{\text{intercept}} < 0.001$ $P_{\text{slope}} < 0.001$, $r^2 = 0.989$, RMSE = 0.02, n = 275; distance in 2006 (m) = 1.56 + 0.76 × neighbor rank, $P_{\text{intercept}} < 0.001$ $P_{\text{slope}} < 0.001$, $r^2 = 0.990$, RMSE = 0.03, n = 239. Distances to the nearest gap were 60 and 57 m in 1997 and 2006, respectively. These

relationships are linear over most ranks, but were slightly curvilinear for very large ranks (Fig. 3.6). This is due to edge effects and the irregular shape of old-growth forest at La Selva (Fig. 3.1), which requires farther distances to observe the *n*th nearest gap than would be expected in a region of contiguous forest. Randomization tests demonstrate that the mean distance to the *n*th nearest gap was shorter than expected for a randomly distributed sample over distances of a few hundred meters, but not different from spatial randomness at larger distances and most of the study area up to the maximum observed distances of 2.7 km (dashed lines, Fig. 3.6).

A larger fraction of the landscape occupied sites < 2 m in 1997 than in 2006 (Table 3.2), but the normalized distribution of gap sizes identified using LiDAR was similar between years (Fig. 3.6). There were 250 gaps within 445 ha of old-growth forest in 1997 and 222 gaps in 2006 (mean densities of 0.56 and 0.49 gaps · ha^{-1} respectively). The size distributions of gaps identified using LiDAR had means of 43.5 m^2 and 37.8 m^2, in 1997 and 2006 respectively. Correlation coefficients relating gap size to topographic slope and predicted soil P were not significantly different from zero in 1997 or 2006 (Table 3.3).

Validation

There was a strong positive relationship between the proportion of vegetation height < 15.00 m identified using LiDAR and field measurements: proportion from LiDAR = 0.134 + 0.736 × proportion from field measurements, $P_{intercept} < 0.001$ $P_{slope} < 0.001$, $r^2 = 0.856$, RMSE = 0.029, n = 18 (Fig. 3.7). For gaps identified using field measurements, mean area was 36.7 m^2 (Table 3.4). This is similar to the mean gap size identified using 2006 LiDAR data (37.8 m^2). There were 30 gaps identified within 18 0.5 ha plots using field methods. Comparison of size

frequency distributions of Brokaw gaps from field and 2006 LiDAR data showed that the proportions of gaps of smaller sizes within plots was representative of their abundance throughout the landscape, although gaps > 125 m^2 were not represented within field data. Simulations demonstrate that the absence of gaps > 125 m^2 within plots is a consequence of the smaller area sampled (9 ha versus 445 ha), not systematic bias, because confidence intervals overlap the values observed within plots and large gaps are rare (Figs. 3.6, 3.7).

Discussion

Persistent disturbance figures prominently in the dynamics of this forest (Fig. 3.3). Although we expected to observe canopy height changes from upward height growth and mortality, substantial dynamics occurred throughout all heights in the canopy. Most gaps were produced by vegetation below the main canopy height, and not by tall canopy trees. Many height losses were not severe enough to form gaps < 2 m. Despite this high frequency of height loss and regeneration, our analysis demonstrates consistency in the sizes and spatial properties of forest disturbance (Fig. 3.6), and suggests that changes in canopy height during 8.5 years were very close to the steady-state equilibrium expectation (Fig. 3.5).

Gap sizes and neighbor distances followed power-laws at La Selva, with slopes that were statistically indistinguishable between years (Fig. 3.6). If species are adapted to the prevailing disturbance regime (Denslow 1980; Hubbell & Foster 1986a), there should be selection for long-distance dispersal. Ecologists have studied seed dispersal many times. One of the most consistent observations is that most seeds fall beneath the crown or near the parent tree. Only a

small fraction of seeds disperses longer distances (Jones *et al.* 2005; Hardesty *et al.* 2006). However, locations and frequencies of gaps at La Selva demonstrate that dispersal must occur over at least several hundred meters just to encounter a small number of canopy gaps (Fig. 3.6). This indicates that selection could favor individuals traveling long distances from their maternal parent, because these individuals would be more likely to encounter conditions favorable to establishment and regeneration. This hypothesis generates predictions for the spatial distribution of seedlings. If selection for long-distance dispersal is occurring, seedlings should establish at farther distances from the maternal parent than expected, given the density of seed dispersal. Evidence of selection for long-distance dispersal will require demonstrating that Janzen-Connell mechanisms are not responsible for patterns of seedling establishment, as similar patterns could be produced under the Janzen-Connell hypothesis, albeit due to a fundamentally different process (Janzen 1970).

We can use the power-law gap-size relationships to predict the abundance very small openings in the forest canopy. Small canopy openings, such as interstitial spaces between branches or tree crowns, are an important source of photosynthetically active radiation to seedlings in deep shade (Chazdon 1988, 1991). Photosynthetic machinery of understory species and tree seedlings may be adapted to harvest light that is available in localized brief periods of intense radiation created by small openings in the canopy (Chazdon 1991). The sizes and frequency of these openings will determine the quality of understory light environments and the density of sunflecks available to understory plants. If the assumption of self similarity holds over ecologically relevant sizes of canopy openings, it would facilitate prediction of understory light environments using LiDAR measurements of canopy structure.

Structure and dynamics

Gap spatial distributions were aggregated over distances of a few hundred meters, but not different from random at larger distances up to 2.7 km (Fig. 3.6). Sizes of canopy gaps were unbiased with respect to topographic slope and predicted soil Phosphorus. These results were surprising, because there are clearly defined responses in forest structure to topography and apparent nutrient limitation (Clark & Clark 2000; Espeleta & Clark 2007), and we expected the smallest gaps to occur on the most fertile sites.

Soil fertility at La Selva is influenced by substrate aging and erosion. Most of the upland landscape is on highly weathered Oxisols and is low in soil P (Kleber *et al.* 2007). Alluvial terraces are of similar origin, but support higher fertility though alluvial deposition (Kleber *et al.* 2007). There is evidence of nutrient rejuvenation on steep slopes within upland landscapes (Porder *et al.* 2006). Plant investment in fine root biomass was higher on low-fertility upland plateaus than on relatively fertile alluvial terraces (Espeleta & Clark 2007). Taken together, these findings indicate that there are plant responses to variability in soil P throughout the landscape, and suggest that Phosphorus availability could limit net primary production. Nonetheless, these effects did not generate detectible patterns in the sizes of disturbance patches < 2 m in height. One mechanism that may explain gap clustering is persistent redisturbance near existing gaps. In tropical moist forest on BCI, gap-edge trees were more likely to fall into existing gaps because of asymmetric crown growth, and newly formed canopy openings occurred closer to existing gaps than expected by chance (Hubbell & Foster 1986b; Young & Hubbell 1991).

The distribution of canopy height was close to the steady-state expectation. This conclusion is based on the dominant eigenvector of the height transition matrix (Appendix A), and comparison of observed and expected height distributions (Fig. 3.5). Differences between the observed and equilibrium conditions were small, and necessarily decreased through time. Equilibrium canopy height under the recent 8.5-year disturbance regime is 20.0 m ± 6.6 m S.D., a height loss of 0.75 m from the observed distribution of canopy height in 1997, and 0.40 m from 2006. However, the steady-state distribution is not simply a shift of a few tens of cm from recent conditions. Height variance was greater in 1997 (7.3 m S.D.) than the equilibrium expectation, a finding that is consistent with increased rates of tree mortality observed during the 1997-98 ENSO (D. B. Clark, pers. comm.), which was five months underway at the time of LiDAR data collection in 1997 (US National Weather Service Climate Protection Center). Subcanopy sites will increase in frequency through gap filling, and mean canopy height will decrease at the expense of the tallest forest trees under the recent disturbance regime (Fig. 3.5). This indicates that the tallest forest trees lost height or died during the 8.5-year study, and have not yet been replaced.

Sources of sampling bias

There was a strong relationship between the proportion of canopy height < 15 m identified using field and LiDAR measurements (Fig. 3.7). However, relative to field measurements, LiDAR over-estimated the frequency of low-canopy sites. Reconciling this discrepancy would build confidence in the ability of LiDAR to provide unbiased measurements of canopy height.

The Leica ALS50 collected irregularly-spaced estimates of vegetation height within circular laser pulses of 0.33 m in diameter. Field measurements of canopy height were collected on a

regular 5 m sampling grid by projecting an imaginary 2 × 2 m quadrat on the vegetation directly above each point of measurement. Because of the difficulty of determining exactly which branch or leaf is directly above the point of measurement in the field, holes in the forest canopy that were smaller than the 2 × 2 m quadrat were treated as closed canopy. Thus, field measurements were not capable of detecting canopy openings smaller than 4 m^2 in area, whereas LiDAR observations could penetrate through openings as small as 0.33 m across. In relatively undisturbed plots, canopy gaps were small, whereas plots occupied by large fractions of low canopy contained large disturbance patches (e.g., one or a few large gaps). If differences in sampling account for the discrepancy between LiDAR and field measurements, the magnitude of bias should be most severe in plots that are relatively undisturbed, and should decrease as the magnitude of disturbance increases. This is precisely the pattern observed in our data, and the regression line approaches the one-to-one relationship as the magnitude of disturbance increases (Fig. 3.7). It indicates that differences between field and LiDAR measurements of canopy height can probably be attributed to difficulties obtaining height measurements in the field, rather than LiDAR error.

Conclusion

LiDAR remote sensing is a powerful tool for quantifying the structure and dynamics of tropical forest canopies. Here we have demonstrated this potential by using observations from two points in time to characterize the sizes and spatial properties of canopy gaps, and the dynamics of height loss and regeneration in an old-growth Neotropical rain forest in the Atlantic lowlands of Costa Rica. The results demonstrate that persistent disturbance is a prominent feature of the dynamics of this forest, a finding that is consistent with ground based studies of upward height

growth in regenerating trees (Clark & Clark 2001). Although there were substantial dynamics, the analysis demonstrates consistency in the sizes and spatial properties of Brokaw gaps at large spatial scales, and suggests that height changes were close to the steady-state equilibrium expectation during 8.5 years. Taken together, these findings challenge the view that Neotropical forests are undergoing directional structural changes in response to global change. The rarity and diffuse coverage of Brokaw gaps provides evidence of the necessary conditions for selection for long-distance dispersal. Integrating LiDAR measurements of forest structure and dynamics with other types of remotely sensed data that can provide information on canopy nutrient and water status, and physiological condition of individual trees, promises to open new avenues in basic and applied research.

Acknowledgements

Measurements in the CARBONO plots were partially supported by the TEAM Project of Conservation International, made possible with a grant from the Gordon and Betty Moore Foundation. Support for the TREES project came from the NSF LTREB Program (DEB-0640206). Funding for acquisition of LiDAR data was supported by contributions from the NSF, NASA, University of Maryland, TEAM, and the University of Alberta. This work was partially funded by a DDIG to JRK.

Fig. 3.1. La Selva, Costa Rica. Land use history and locations of field plots and LiDAR coverage. The site has a mixed history of historical landuse, including cleared or developed areas, selectively logged forest, old-growth forest, current and abandoned plantations or pastures, an ecological reserve that is mostly old-growth, second-growth forests, and swamps. LiDAR observations were collected by the FLI-MAP system in 1997 (rectangular area) and by the Leica ALS50 in 2006 (entire area). Analyses here are from the 445 ha of old-growth forest for which LiDAR data from 1997 and 2006 are available. Locations of 18 0.5 ha field-inventory plots are shown as black rectangles.


DEVELOPED
LOGGED
OLD GROWTH
PLANTATION
RESERVE
SECOND GROWTH
SWAMP
1,000
FIELD PLOTS
1997 LiDAR

Fig. 3.2. Canopy height model from LiDAR. The sample is for 9 ha of old-growth forest at La Selva, Costa Rica in 1997. Data are from the FLI-MAP system, and each pixel is 0.33 × 0.33 m. Canopy height models in 1997 and 2006 were resampled to 5 × 5 m for analysis of gap locations and canopy dynamics. Pixels ≤ 2 m in height (Brokaw gaps) are distinguished in red.

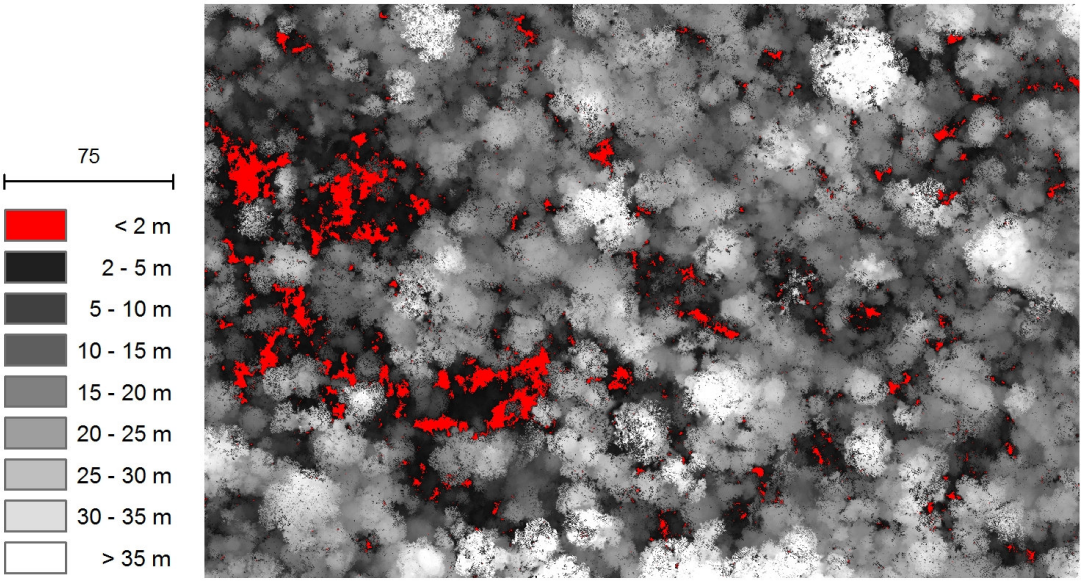
75
< 2 m
2 - 5 m
5 - 10 m
10 - 15 m
15 - 20 m
20 - 25 m
25 - 30 m
30 - 35 m
> 35 m

Fig. 3.3. Canopy height transitions in an old-growth tropical rain forest. Data are probabilities of entering (left column) or exiting (right column) a given 1 m height class, denoted by text label and vertical dashed line. Probabilities were estimated using 177,855 canopy height changes on a 5 m sampling grid during 8.5 years using LiDAR remote sensing. Many disturbances did not produce gaps in the forest canopy, and most gaps were produced by vegetation below the height of the main canopy.

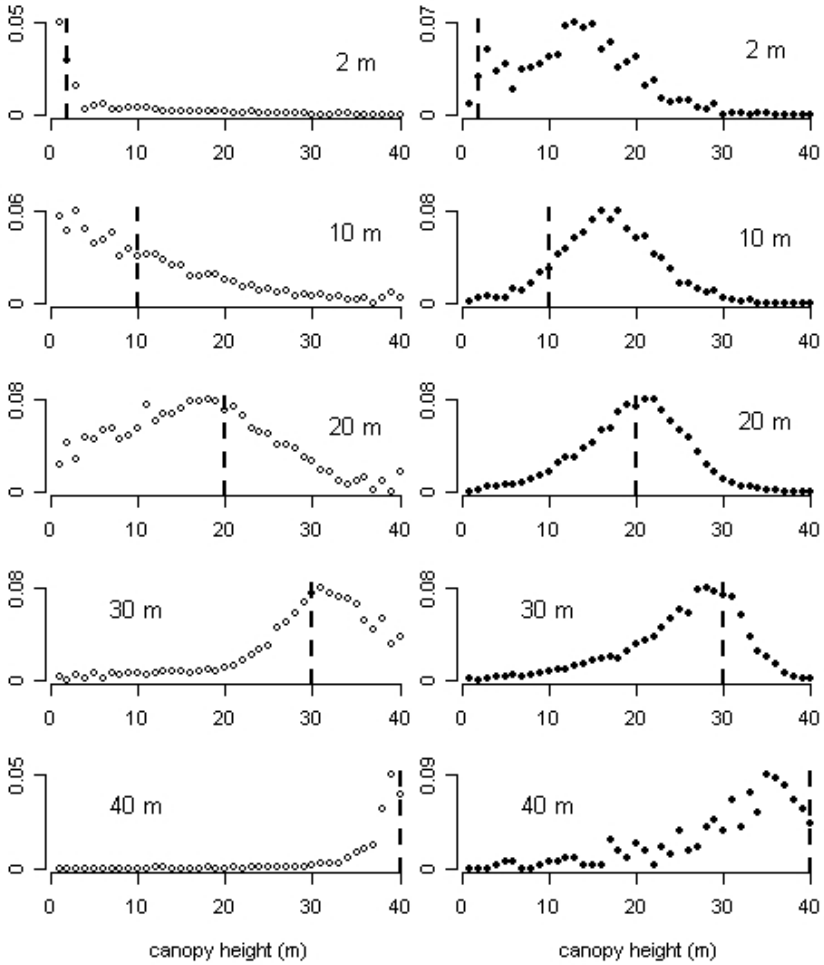
2 m
2 m
10 m
10 m
20 m
20 m
30 m
30 m
40 m
40 m
canopy height (m)
canopy height (m)

Fig. 3.4. Canopy dynamics in an old-growth rain forest. Change in height (m) between 1997 and 2006 was associated with canopy height in 1997 ($P < 0.001$, $r^2 = 0.281$). Low-canopy sites increased and tall sites had height loss. The figure shows a random sample of 2,000 points, but the relationship was estimated using 177,855 observations made using LiDAR. The vertical and horizontal dashed lines indicate the mean canopy height in 2006 (20.4 m) and zero net change, respectively.

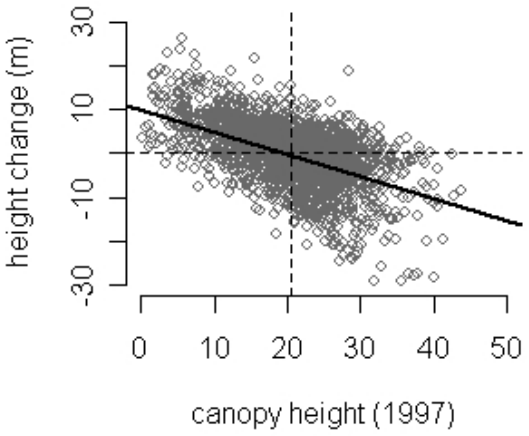
height change (m)
30
10
-10
-30
0
10
20
30
40
50
canopy height (1997)

Fig. 3.5. Distribution of canopy height at La Selva, Costa Rica. The distribution of canopy height in 1997 (left panel) was close to the steady-state expectation (dots in both panels) projected using height changes over 8.5 years. By 2006 (right panel), subcanopy sites increased in frequency through gap filling, and mean canopy height decreased at the expense of the tallest forest trees.

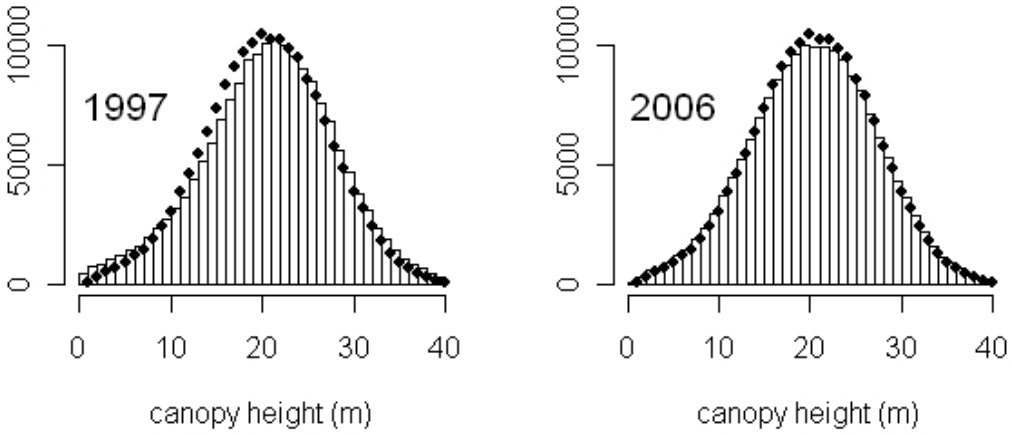
1997
2006
0
5000
10000
0
10
20
30
40
canopy height (m)

Fig. 3.6. Power law scaling relationships in canopy gap disturbance. The expected number of gaps decreases linearly as a function of gap size on log-log axes (top panels). The distance to the *n*th nearest gap increases linearly as a function of rank *n* on log-log axes (bottom panels). Slopes of relationships were statistically indistinguishable between data from 1997 and 2006. Dashed line in bottom panels is the expected distance to the *n*th nearest gap under complete spatial randomness and indicates that gaps are aggregated over distances of a few hundred meters. Curvilinearity associated with very large ranks in the bottom panels is due to edge effects.

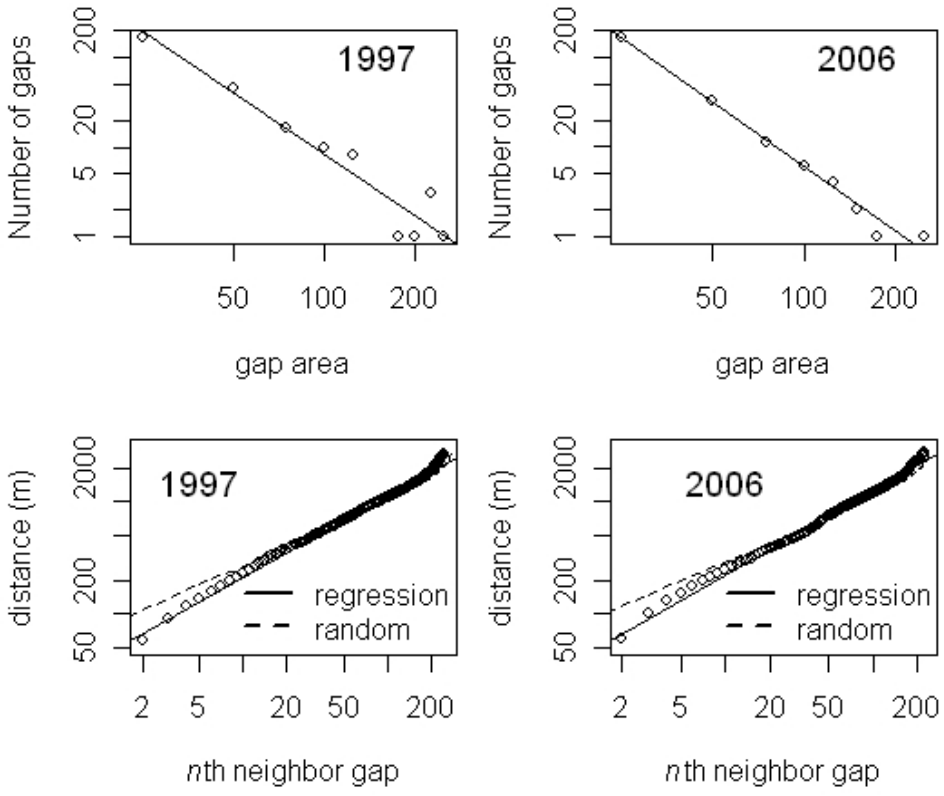
Number of gaps
1
5
20
200
1997
50
100
200
gap area
Number of gaps
1
5
20
200
2006
50
100
200
gap area
distance (m)
50
200
2000
1997
regression
random
2
5
20
50
200
nth neighbor gap
distance (m)
50
200
2000
2006
regression
random
2
5
20
50
200
nth neighbor gap

Fig. 3.7. Estimates of tropical forest structure from LiDAR. The proportion of canopy height measurements < 15.00 m identified using field sampling and LiDAR data is highly correlated within 18 permanent inventory plots (left panel). The size frequency distributions of gaps in the forest canopy identified using LiDAR or field measurements are statistically indistinguishable, but gaps > 125 m^2 were not represented in plots (right panel).

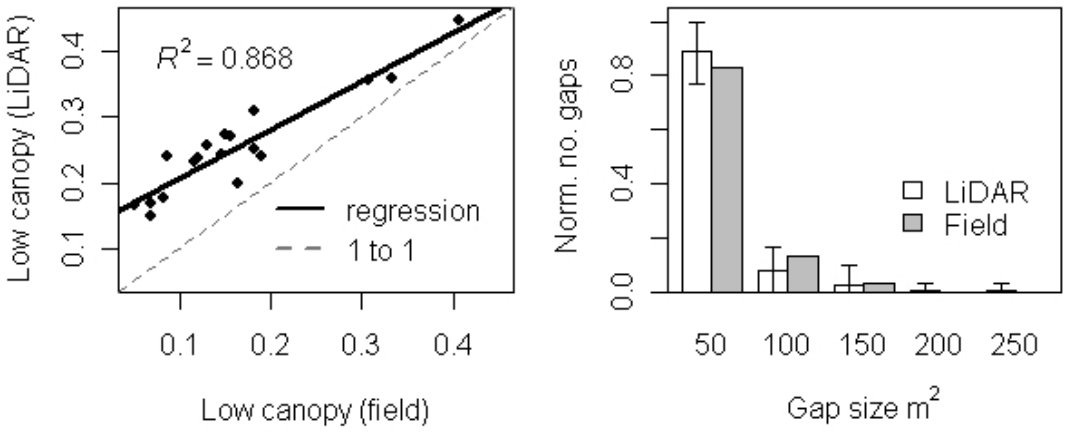
Low canopy (LiDAR)
0.1
0.2
0.3
0.4
R^2 = 0.868
regression
1 to 1
0.1
0.2
0.3
0.4
Low canopy (field)
Norm. no. gaps
0.0
0.4
0.8
LiDAR
Field
50
100
150
200
250
Gap size m^2

Table 3.1. A subset of the canopy height transition matrix. Numbers are transition probabilities from the column to row height class over 8.5 years. Estimates are from 177,855 canopy height changes observed in 445 ha using LiDAR remote sensing.

	Canopy height class in 1997 (m)								
2006	< 2	2 – 5	5 – 10	10 – 15	15 – 20	20 – 25	25 – 30	30 – 35	35 – 40
< 2	0.046	0.010	0.004	0.003	0.002	0.001	0.001	0.000	0.000
2 – 5	0.121	0.053	0.023	0.014	0.013	0.010	0.007	0.005	0.003
5 – 10	0.183	0.163	0.114	0.080	0.060	0.045	0.032	0.024	0.021
10 – 15	0.320	0.321	0.298	0.251	0.179	0.115	0.076	0.047	0.039
15 – 20	0.217	0.279	0.336	0.373	0.344	0.240	0.147	0.082	0.060
20 – 25	0.077	0.125	0.166	0.209	0.291	0.350	0.274	0.170	0.105
25 – 30	0.031	0.039	0.051	0.059	0.094	0.199	0.327	0.304	0.191
30 – 35	0.005	0.008	0.008	0.010	0.014	0.035	0.122	0.294	0.334
35 – 40	0.000	0.001	0.000	0.001	0.001	0.003	0.013	0.072	0.247

Table 3.2. Canopy height dynamics in an old-growth tropical rain forest. Numbers are the proportion of 177,855 canopy height estimates on a 5 m grid within each height class in 1997 and 2006.

	Canopy height class (m)								
Year	< 2	2 – 5	5 – 10	10 – 15	15 – 20	20 – 25	25 – 30	30 – 35	35 – 40
1997	0.007	0.018	0.056	0.125	0.237	0.276	0.187	0.071	0.019
2006	0.002	0.013	0.055	0.149	0.254	0.269	0.175	0.066	0.015

Table 3.3. Correlation coefficients between gap size and slope or soil P.

	Pearson's *r*			
	1997	*P* (1-tailed)	2006	*P* (1-tailed)
slope	0.017	0.609	-0.099	0.069
Phosphorus	-0.058	0.190	0.092	0.909

Table 3.4. Cumulative percent of the number of gaps and area in gaps.

	Gap area (m^2)					
	50	100	150	200	250	300
cumulative percent of gaps (1997)	84	96	99	99	100	100
cumulative percent of area (1997)	66	83	91	94	100	100
cumulative percent of gaps (2006)	89	96	99	99	100	100
cumulative percent of area (2006)	76	90	97	98	100	100
cumulative percent of area (field)	83	97	100	100	100	100
cumulative percent of area (field)	69	92	100	100	100	100

CHAPTER 4

POTENTIAL AND LIMITATIONS OF HYPERSPECTRAL IMAGING TO ESTIMATE UPPER-CANOPY FOLIAR NITROGEN IN A LOWLAND NEOTROPICAL RAIN FOREST[3]

[3] Kellner, J.R. Unpublished manuscript.

Introduction

Nitrogen is a fundamentally important component of ecosystems. In plant leaves it mediates rates of mass-specific photosynthesis (A_{max}), and is thus a central determinant of global net primary production (NPP). Differences in the content of foliar N among tropical rain forest canopy tree species define the familiar life-history axis from 'shade tolerance' to 'gap dependence', and because light is the most limiting essential resource to regeneration in the forest understory, the content of N within plant leaves should determine rates of survival and growth, with implications for competition among neighbors and the likelihood of canopy recruitment.

In this chapter, I summarize the status of an effort to estimate foliar N within tree canopies using airborne hyperspectral imaging over a tropical rain forest in the Atlantic lowlands of Costa Rica. The objectives are to describe and interpret variation in canopy N throughout a tropical rain forest landscape, and to test whether the growth and performance of individuals can be predicted using their nutrient status relative to neighbors. The study encountered several limitations that have preempted useful estimates of canopy N to be made. However, before describing the approach and concluding with a way forward, it is useful to document the observations that motivated the original proposal.

Background

The tropical wet forest at La Selva Biological Station contains > 300 species of trees, most of which occur at very low population densities (<<1 individual $\cdot$ ha^{-1}). This observation is a

hallmark of tropical biodiversity (Wallace 1878; Hubbell 1979), and has been the subject of long-term speculation. How such diversity is generated, structured and maintained, and why differences occur between temperate and tropical biomes is, on the one hand, one of the most obvious natural history observations to anyone who has visited tropical and temperate biomes. One the other hand, we lack definitive answers to these questions, which remain at the forefront of debate in ecology and evolutionary biology (Hubbell 2001; Jablonski *et al.* 2006).

Classical work has demonstrated the difficulty with which > 1 species can be made to coexist when the number of resources is limiting (Gause 1934; Tilman 1980). It has also been shown that natural selection can produce divergence of characters, such that strong competition between species is preempted (Darwin 1859). Evidence for character displacement in plant population has been difficult to obtain. Unlike most animals, plants live their lives rooted to the spot, and do not move. All plants compete for the same relatively small set of essential macronutrients, water, light, and space, and it is challenging to think of ways in which these resources could be uniquely partitioned among hundreds of coexisting species. Nonetheless, the idea that niche differences ultimately determine the distribution and abundance of species has remained prominent. Under this view, traits of importance to the way a species acquires resources (i.e. functional traits, McGill *et al.* 2006) should differ to a corresponding degree, a process known as limiting similarity (Hutchinson 1961, MacArthur and Levins 1967, Shipley et al. 2006). In plant communities, where interactions between individuals occur in a spatial setting, this hypothesis generates predictions for the spatial distribution of plant performance with respect to neighboring individuals. Plants with traits that are similar to their neighbors

should perform relatively poorly, while individuals whose traits are distinct, and thus facilitate a different strategy of resource acquisition, should perform relatively well.

The hypothesis of limiting similarity does not deny the existence of other processes, some of which may generate alternative predictions. Habitat filtering occurs when resources are patchily distributed in space, and individuals adapted to particular resources are clustered within suitable habitat patches. Familiar examples in tropical rain forest trees are species with topographic or edaphic biases (Clark *et al.* 1998; Webb & Peart 2000; Harms *et al.* 2001). Although habitat filtering would produce spatial clustering of species traits to the extent that individuals are tracking physiochemical gradients in the environment, performance within habitat patches should still be influenced by the intensity of competition with neighbors, and the hypothesis of limiting similarity should still operate. Testing the hypothesis of limiting similarity is an exercise in calculating the strength of evidence in support of the hypothesis, rather than attempting to reject all hypotheses but one.

The hypothesis of limiting similarity has been an important contributor to ecological thought for more than 40 years, but its ability to explain patterns of abundance in tropical tree communities has been equivocal. There are two reasons for this. First, a rigorous test in plant communities requires information on which characters dictate growth and performance of individuals, and identifying the differences in those characters that permit individuals to have fitness advantages. Such information may sometimes be available in animal communities, but in plants it is far from obvious. For example, no one would dispute that the long and decurved bill of the Hawaiian honeycreeper, I'iwi, (*Vestiaria coccinea*) facilitates better access to sources of nectar deep within

Lobeliod flowers, and it cannot be disputed that the stout and pointed bill of the ‘Akiapola’au (*Hemignathus munroi*), or Hawaiian Woodpecker, allows that species to obtain insects and nectar that are not available to the I’iwi. Because Hawaiian honeycreepers are related by common decent to a finch-like ancestor, and co-occur within Hawaiian forests, bill morphologies are strong evidence that character displacement has occurred, and that it operated on strategies of food acquisition, and possibly mate attraction (Freed *et al.* 1987). Yet, all plants are green. To be sure, co-occurring plant species differ in traits that should have fitness consequences, and there is clear evidence that plants can respond to underlying gradients in resources or toxins in ways that are advantageous to growth and survival (e.g., Schat *et al.* 1996; Treseder & Vitousek 2001). However, we know but little of the mechanisms through which such adaptation occurs, and next to nothing of whether these mechanisms are responsible for patterns of community assembly in nature.

Second, strong inferences in population and community dynamics of tropical rain forest trees are restricted to the earliest life stages (seeds, seedlings, saplings, and sub-adult trees for some relatively ‘common’ species). Recruitment to the canopy can take decades or centuries to occur (Clark & Clark 2001), and because adults for most species are rare, direct observation of adult dynamics has not been possible (but see chapter two). This is a striking difference from animal ecology, where researchers sometimes ignore juveniles entirely, and consider only on the dynamics of individuals of reproductive age, or even reproductive females. There are important differences between plants and animals, and reasons to suspect that the juvenile life stages may be more relevant to understanding population dynamics and coexistence in plant populations (Janzen 1970). However, our inability to observe directly the dynamics of the component of tree

populations with positive fitness, or to identify characteristics that determine whether a given juvenile will recruit to the adult life stage, is a profound limitation that cannot be overstated. Thus, inferences about the importance of processes that occur early in growth and development, such as regeneration niches, life history tradeoffs, and seed to seedling density dependence ultimately depend on their ability to influence the composition of canopies, but our capacity to demonstrate that such processes actually do influence the composition of canopies has been critically limited. If life-history differences, regeneration niches, or density dependence do not determine which individuals will recruit to the canopy, their role in structuring tropical tree communities would be in doubt.

Remote sensing of community dynamics

I take a different approach to evaluating the consequences of trait differences on species interactions. By using airborne imaging spectroscopy (also called 'hyperspectral remote sensing') it is possible to quantify the biophysical and chemical properties of vegetation throughout very large areas (Asner *et al.* 2004; Asner & Vitousek 2005). These estimates can be integrated with LiDAR observations (chapter three), which provide finely grained measurements of canopy height and ground elevation, to interpret patterns in the structure and dynamics of vegetation. With estimates of the concentrations of chemical constituents made using remote sensing, it becomes possible to directly observe dynamics within forest canopies. Because foliar N is a strong determinant of A_{max}, and is likely to define a primary axis of life-history variation, it should provide a strong test of the hypothesis of limiting similarity throughout a tropical rain forest landscape.

Imaging spectroscopy

Imaging spectroscopy is the measurement of reflected solar radiation within contiguous, narrow channels of the electromagnetic spectrum between 450 and 2500 nm (Ustin *et al.* 2004; Asner 2008). When radiation is reflected by plant tissues, known properties of the spectral response to physiological processes, structure, and biochemistry can be used to identify species (Clark *et al.* 2005; Carlson *et al.* 2007), to estimate differences in canopy water and NPP associated with drought stress (Asner *et al.* 2004) and to quantify concentrations of canopy nutrients and pigments within foliar tissue (Smith 2002; Asner & Vitousek 2005; Ollinger 2005; Asner 2008). Throughout the visible wavelengths (VIS, 400 – 700 nm), reflectance is dominated by chlorophyll and other leaf pigments (Asner 2008). Chlorophyll-a has fundamental absorptions centered at 430 and 660 nm, and chlorophyll-b has fundamental absorptions at 460 and 640 nm (Curran 1989; Asner 2008). There is an abrupt increase in reflectance of green vegetation at approximately 700 nm (the 'red edge', Fig. 4.1) and radiation is strongly reflected throughout the NIR (700 – 1300 nm). Water has absorption features centered at 970, 1140, and 1940 nm. Leaf morphology and structure are important contributors to reflectance throughout the NIR and short-wave infrared (SWIR, 1300 – 2500) regions, including leaf hairiness, thickness, presence of air spaces, lignin and cellulose contents (Curran 1989; Asner 2008).

Although features of the spectral response can be associated with biomechanical properties of vegetation, it is important to note that there is no particular wavelength or spectral feature of foliar tissue that relates directly to the content of foliar N, or any other biomechanical property (Asner 2008). Direct relationships can be established using pure substances under laboratory conditions, but in practice, the reflectance of different components of vegetation combine with

geometric properties of canopies to generate the observed spectral response. Most N in plant leaves is bound in the enzyme Rubisco, which is strongly correlated with the abundance of chlorophyll, and therefore N content in leaves can be correlated with absorption features in the visible wavelengths. Nitrogen in protein has absorption features centered at 1510, 1940, 2180, and 2350 nm (Curran 1989). Other sources of N are not expressed directly in the spectral response, but covary with traits that do produce characteristic features (Reich *et al.* 1997), such as SLA and leaf water content. Thus, the sensing of N or other properties of foliar vegetation using remotely sensed data characterizes a suite of physical and biological variables that can be very highly correlated with the quantity of N from field measurements (Asner 2008).

Hyperspectral data

The HYperspectral Digital Imaging Collection Experiment (HYDICE) is an airborne imaging spectrometer that collected data over La Selva Biological Station on March 30, 1998. The HYDICE sensor measured radiance within 210 channels covering the 400 to 2500 nm region of the electromagnetic spectrum (Basedow *et al.* 1995; Clark *et al.* 2005). La Selva data were collected from 3.17 - 3.20 km altitude, producing a pixel resolution of 1.6 m at ground elevation, in which individual tree crowns are clearly resolved (Clark *et al.* 2005). The data were georeferenced and orthorectified using a 0.33 m LiDAR canopy height model (described in chapter three and in CLARK ET AL 2005), and atmospherically corrected to surface reflectance using ACORN (ImSpec LLC). Noisy bands < 437 nm, and bands in the 1313 – 1466 nm and 1771 – 1994 nm regions were removed from the analysis. A full description of image processing and calibration is in Clark et al. (Clark *et al.* 2005)

Estimation of canopy N

I used partial least squares regression (PLS) to predict the abundance of upper-canopy N using observations from HYDICE. PLS collapses high-dimensional data into a smaller number of independent variables, and finds the least-squares estimates of parameters that relate a vector of observations to a matrix of predictors with the highest explanatory power (normally based on r^2). It has been used extensively for estimation of leaf N from spectroscopic data (e.g., Smith 2002; Ollinger 2005). A limitation to the use of PLS is that it is necessarily site and data-set specific. Like other forms of eigen analysis, the most important factors in a PLS model may lack generality or physical interpretation, and the method is therefore prone to over fitting.

To evaluate the ability of PLS regression to predict upper canopy foliar N using HYDICE, I employed a 'leave-one-out' cross-validation. In this approach, one field estimate of canopy N is deleted from the data, and the empirical relationship is estimated using the remaining $n - 1$ observations. The model is then used to predict the value of the omitted observation. This process is repeated for all field observations and the relationship between observed and predicted field N is assessed.

The PLS model was parameterized using field measurements of upper canopy foliar % N that were collected between June 2003 and June 2005. Leaf samples were obtained from 22 sites by collecting upper-canopy vegetation using a mobile scaffolding tower. The location of each tower was established a priori using stratified random sampling within old-growth forest to account for underlying gradients in soil Phosphorous (P) and topographic slope. Previous work has demonstrated that soil P probably limits productivity at La Selva (Espeleta & Clark 2007), and

that nutrient rejuvenation occurs on steep slopes (Porder *et al.* 2006). Thus, the sampling regime accounted for the dominant sources of variation in nutrient limitation throughout the landscape. At each sampling location, a scaffolding tower was constructed in sections of 2.45 m × 1.86 m × 1.86 m (L × W × H). The number of sections at each site varied depending on the maximum vegetation height at the particular site (from one to twenty-four sections). Within each tower section, all vegetation was harvested and processed. Clark et al. (2008) described the vertical and horizontal distribution of LAI, and Cavaleri et al.(2006) provide an analysis of woody CO_2 efflux. Cavaleri et al. (2008) quantified foliar and ecosystem respiration, and demonstrated that small temperature fluctuations can dictate changes in carbon balance for the forest at La Selva. For the purposes of this study, foliar N was estimated from randomly selected leaves within the top section of each tower sample using a LECO TruSpec CN Determinator at Colorado State University (LECO Corporation, St. Joseph, MI, USA). The location of each tower was established using differentially-corrected GPS. To associate field measurements of canopy N with reflectance, I extracted the 161 reflectance measurements at the location of each tower using a geographic information system.

PLS regression was applied to the estimates of foliar N from the top section of each tower, as opposed to the entire column of vegetation sampled. This is appropriate because the effective photon penetration depth (EPPD) of radiation in the 400 - 2500 nm range is strongly wavelength dependent (Asner 2008). Knowing precisely the canopy volume to which estimates of N from remote sensing apply will depend on the specific absorption features that most strongly predict field measurements. In general, N is expressed directly by features with shallow EPPD (< 2 LAI

units). At La Selva, this corresponds to the upper-most portion of the vertical tower section and canopy (Clark *et al.* 2008).

Results and Discussion

Field samples of upper canopy foliar N ranged from 1.22 – 3.00 %, with a mean of 2.21 ± 0.09 S.E. PLS regression failed to predict field measurements of foliar N at La Selva with reasonable explanatory power (Fig. 4.2). I considered regression models with up to 10 factors. Although the relationship became statistically significant using ≥ nine factors, the highest coefficient of determination was 0.15 (ten factors), and I conclude that the ability of 1998 HYDICE observations to predict field measurements of upper canopy % N collected between 2003 and 2005 is poor.

There are at least three non-independent reasons why 1998 HYDICE observations could have been unable to predict field measurements of leaf N at La Selva. (1) The HYDICE sensor lacks the sensitivity of other imaging spectrometers that have been used to predict N with high accuracy. (2) Geolocation errors may have prevented correct association between reflectance spectra and field measurements. (3) The dynamics of the forest canopy and foliar N changed through time, and too much time had passed (5 – 7 years) between collection of image data and field measurements for any relation that existed to remain strong.

Precision of HYDICE

The HYDICE system does not achieve the high precision of current-generation imaging spectrometers such as NASA's Airborne Visible and Infrared Imaging Spectrometer (AVIRIS), which has demonstrated capacity to predict field measurements of upper canopy foliar N with high accuracy (e.g., Asner & Vitousek 2005; Martin *et al.* 2008). However, this is unlikely to account for the inability of HYDICE to predict field measurements at La Selva. I examined spectral responses using HYDICE reflectance observations within crowns of four species of trees in the upper canopy, and one standing dead individual of unknown species identity in a tree-fall gap (Fig. 4.1). Three of the four living trees were mapped in the field as part of a long-term demographic study (the TREES project, Clark & Clark 1992), and field work has been conducted to associate observable crowns using remotely sensed data with known stems on the ground (Clark *et al.* 2005, J. Kellner, unpublished data). The four species are *Balizia elegans*, *Dipteryx panamensis*, *Lecythis ampla*, and *Ceiba pentandra*. I haphazardly selected a single pixel within the crown of each tree for the purposes of illustration (Fig. 4.1). The standing dead tree is a conspicuous feature that I first observed within LiDAR imagery from the FLI-MAP system, and subsequently visited in the field in 2005 because I wondered what it was.

This simple analysis demonstrates that there are clear differences in spectral responses between the species, and between dead woody tissue and living foliar tissue (Fig. 4.1). The red-edge at 700 nm and water absorption features at 970 and 1140 nm are clearly resolved in each vegetation sample, but are absent from the standing-dead tree. Reflectance in the SWIR is also higher for the standing-dead sample than in any of the living trees, which is consistent with the dominance of wood reflectance by lignin.

Examination of the spectral responses in Fig. 4.2 is instructive, because it demonstrates that features correlated with biomechanical properties of vegetation, and foliar N in particular, appear to be well resolved by the HYDICE data. One way to determine which regions of the electromagnetic spectrum are associated with foliar N in a given sample is to examine a plot of the factor weights from PLS regression as a function of wavelength. Regions of the spectrum associated with absolutely large coefficients contain information on the content of foliar N. Martin et al. (2008) used data from AVIRIS to estimate upper canopy foliar N at five sites in eastern North America. The coefficient of determination relating remote predictions to field measurements for all sites combined was 0.83. Their plot of factor weights as a function of wavelength shows that the highest weights were associated with features that are present in the HYDICE data. Namely, the most important determinants of foliar N from AVIRIS were a negative relationship near the red edge (700 nm), and strong positive relationships between foliar N and water absorption features in the NIR.

Geolocation accuracy

Geolocation accuracy is also unlikely to account for the poor ability of HYDICE to predict upper canopy leaf N at La Selva. Locations of field sampling within towers were established using differentially corrected GPS with sub-meter accuracy, and HYDICE image data were orthorectified using a 0.33 m LIDAR canopy height model. Evidence that the LiDAR canopy height model is referenced precisely comes from comparison to an independently acquired sample of LiDAR data from the Leica ALS50 (chapter three). The mean absolute difference between horizontal locations of conspicuous features that were observed in FLI-MAP and Leica digital canopy models was 1.43 m ± 0.86 m S.D., which is less than the side length of a HYDICE

pixel. Even if the specific HYDICE pixel from which field measurements were collected had been shifted by several meters, values of N in the upper canopy should be correlated over small distances, at least within individual crowns.

Canopy dynamics

The most plausible explanation for the inability of HYDICE to predict field measurements of foliar N is that the forest at La Selva is dynamic, and contents of foliar N within vegetation are likely to change through time. In chapter three, I used LiDAR observations from 1997 and 2006 to quantify height changes throughout old-growth forest. I found that most sites throughout the old-growth landscape experienced large increases or decreases in height; changes in height of > 5 m occurred throughout 43% of the old-growth landscape during an 8.5 year interval. The high frequency of disturbance in the canopy indicates that many features of the canopy that were present when the HYDICE data were acquired in 1998 no longer remain, so that field measurements from 2003 - 2005 may not be associated with the same canopy objects that were present in 1998. Even if structural changes do not occur, the dynamics of foliar N within individual crowns could weaken a relationship between spectroscopic and field measurements that are collected at different points in time. Wood et al. (2005) monitored contents of N and P in leaf litter within old-growth forest at La Selva between 1998 and 2001. They documented significant changes in absolute foliar % N. At the beginning of their study mean % N in leaf litter was about 2%. It then trended downward to ~ 1.4% by 2001. Though small in magnitude, a change of even 0.5 % in the content of foliar N is approximately 25 % of the mean value observed using towers samples.

A way forward

The finding that spectral responses from HYDICE contain absorption features that were associated with foliar nitrogen in a separate study is cause for optimism. It is likely that foliar N can be retrieved from the 1998 HYDICE data using a different approach. One method would be to assign values of N to pixels in the HYDICE image by associating the reflectance spectrum of each pixel to the closest match in a reference library of vegetation spectra with known properties. For example, if the least-squares match for a pixel within the crown of a *D. panamensis* had 1.5 % foliar N, that value could be assigned to the given *D. panamensis* pixel. Validation could be accomplished by establishing independent training and testing sets, or by using a leave-one-out cross validation. A similar procedure was implemented by Asner and Vitousek (2005) to predict upper canopy foliar N in a Hawaiian montane rain forest. The coefficient of determination between field and remote measurements was 0.91 (Asner & Vitousek 2005).

Summary

Quantifying biochemical properties of rain forest canopies is possible using hyperspectral imaging, and can help to test hypotheses about forest dynamics through direct observation of canopy trees throughout large areas. However, using observations from the airborne HYDICE sensor and field measurements, PLS regression models were unable to predict upper canopy foliar N with precision or accuracy for tropical wet forest at La Selva, Costa Rica. This probably reflects underlying changes in the dynamics of vegetation and contents of foliar N between the time of collection of image and field data, rather than inadequate information contained within spectroscopic measurements. Absorption features associated with biomechanical properties of plants are clearly resolved in spectroscopic measurements using HYDICE, including features

that have been associated with foliar N using AVIRIS at other sites. A sampling procedure that associates vegetation spectra from large databases of tropical plants with HYDICE observations may provide robust estimates of upper canopy foliar N at La Selva.

Acknowledgements

I am grateful to Mike Ryan and Molly Caveleri for generously providing me with access to their field measurements of canopy N from the towers project. Georeferencing, orthorectification, and atmospheric correction of HYDICE data were conducted by Matthew Clark, who also shared data on locations of tree crowns that were distinguishable using HYDICE. This project was supported by a Doctoral Dissertation Improvement Grant from the National Science Foundation to James R. Kellner and Stephen P. Hubbell.

Fig. 4.1. Optical reflectance for rain forest canopy trees. Plots show spectral responses for four species and a standing dead individual of unknown identity. Each sample is the spectral response within a single haphazardly selected pixel representing green vegetation or standing dead wood. The data are from hyperspectral imaging collected using the HYDICE sensor over La Selva Biological Station during March, 1998. Biophysical properties of plant wood and leaf tissues are clearly resolved.

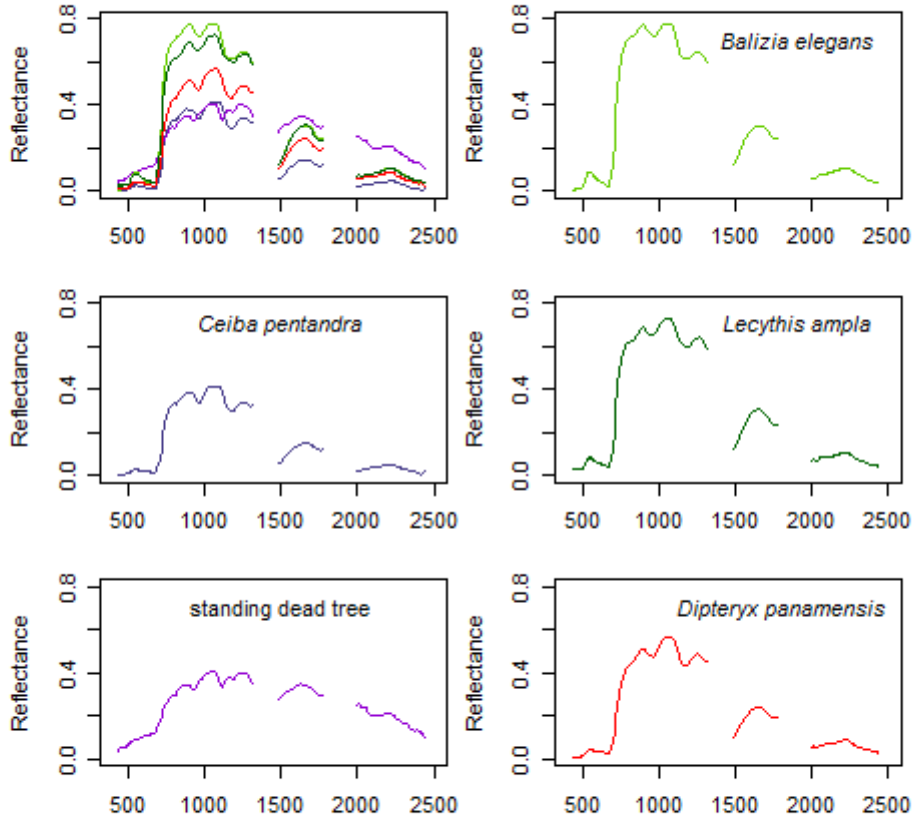
Reflectance
0.0
0.4
0.8
500
1000
1500
2000
2500
Balizia elegans
Ceiba pentandra
Lecythis ampla
standing dead tree
Dipteryx panamensis

Fig. 4.2. Upper canopy foliar N from 22 vertical tower samples of vegetation within old-growth rain forest. Data are from the top 1.86 m of the canopy at each tower location. PLS regression was unable to predict field measurements of upper canopy foliar N ($P = 0.306$, $r^2 = 0.005$). The line denotes a 1:1 relationship.

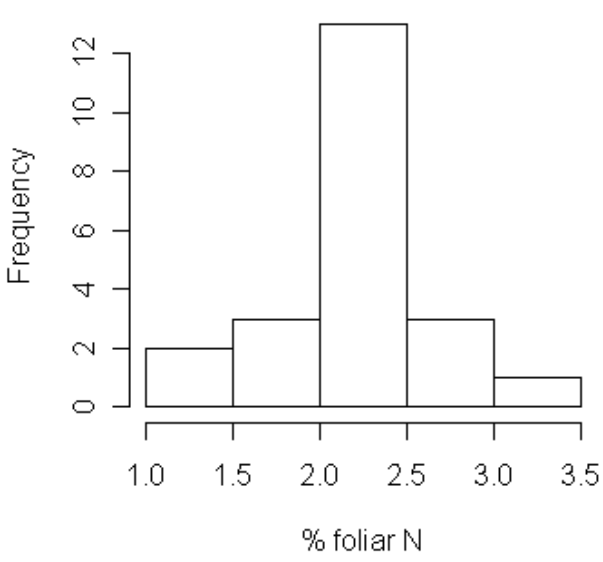
Frequency
0
2
4
6
8
10
12
1.0
1.5
2.0
2.5
3.0
3.5
% foliar N

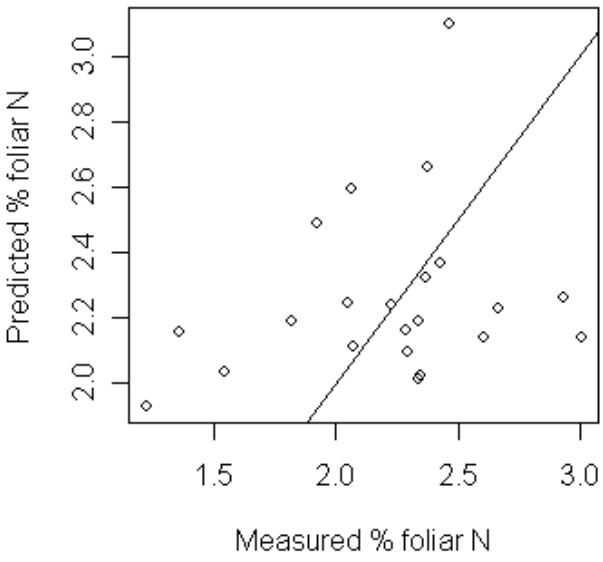
Predicted % foliar N
2.0
2.2
2.4
2.6
2.8
3.0
1.5
2.0
2.5
3.0
Measured % foliar N

CHAPTER 5

CONCLUDING REMARKS

The landscape perspective of canopy tree populations that is possible using remote observations should provide novel insights and better statistical power to test hypotheses about the drivers of population and community dynamics. This dissertation has demonstrated novel capacity to quantify the essential components of population dynamics for rain forest canopy trees using readily available remotely sensed data, even when detection is imperfect, and without estimating abundance. Although the spectral characteristics of flowering *T. guayacan* were useful in the remote identification of this species, the analytical approach developed here is general and will allow demographic analyses of other canopy tree species using satellite or airborne remote sensing. Widespread monitoring for model organisms is achievable using contemporary satellite observations. Studies should establish which canopy tree species can be reliably sampled by satellite by focusing on periods of spectral distinctness associated with phenological change (Frankie 1974). Larger numbers of species can be monitored using airborne hyperspectral observations, even in the absence of conspicuous phenology (Asner & Vitousek 2005; Clark *et al.* 2005; Castro-Esau *et al.* 2006; Carlson *et al.* 2007).

LiDAR remote sensing is a powerful tool for quantifying the structure and dynamics of tropical forest canopies. Here I have demonstrated this potential by using observations from two points in time to characterize the sizes and spatial properties of canopy gaps, and the dynamics of height loss and regeneration in an old-growth Neotropical rain forest in the Atlantic lowlands of Costa Rica. The results demonstrate that persistent disturbance is a prominent feature of the dynamics of this forest, a finding that is consistent with ground based studies of upward height

growth in regenerating trees (Clark & Clark 2001). Although there were substantial dynamics, the analysis demonstrates consistency in the sizes and spatial properties of Brokaw gaps at large spatial scales, and suggests that height changes were close to the steady-state equilibrium expectation during 8.5 years. Taken together, these findings challenge the view that Neotropical forests are undergoing directional structural changes in response to global change. The rarity and diffuse coverage of Brokaw gaps provides evidence of the necessary conditions for selection for long-distance dispersal. Integrating LiDAR measurements of forest structure and dynamics with other types of remotely sensed data that can provide information on canopy nutrient and water status, and physiological condition of individual trees, promises to open new avenues in basic and applied research.

REFERENCES

Adams J.B., Smith M.O. & Johnson P.E. (1993). Imaging spectroscopy: Interpretation based on spectral mixture analysis. In: *Remote geochemical analysis: Elemental and mineralogical composition* (eds. Pieters CM & Englert PAJ). Cambridge University Press Cambridge, pp. 145 - 164.

Asner G.P. (1998). Biophysical and biochemical sources of variability in canopy reflectance. *Remote Sensing of Environment*, 64, 234-253.

Asner G.P. (2004). Drought stress and carbon uptake in an Amazon forest measured with spaceborne imaging spectroscopy. *Proceedings of the National Academy of Sciences of the United States of America*, 101, 6039-6044.

Asner G.P. (2005). Remote analysis of biological invasion and biogeochemical change. *Proceedings of the National Academy of Sciences of the United States of America*, 102, 4383-4386.

Asner G.P. (2008). Hyperspectral remote sensing of canopy chemistry, physiology and diversity in tropical rainforests. In: *Hyperspectral remote sensing of tropical and subtropical forests* (eds. Kalacska M & Sanchez-Azofeifa GA). Taylor and Francis Group.

Asner G.P., Hughes R.F., Vitousek P.M., Knapp D.E., Kennedy-Bowdoin T., Boardman J., Martin R.E., Eastwood M. & Green R.O. (2008). Invasive plants transform the three-dimensional structure of rain forests. *Proceedings of the National Academy of Sciences of the United States of America*, in press.

Asner G.P., Knapp D.E., Kennedy-Bowdoin T., Jones M.O., Martin R.E., Boardman J.W. & Field C.B. (2007). Carnegie Airborne Observatory: in-flight fusion of hyperspectral

imaging and waveform light detection and ranging (wLiDAR) for three-dimensional studies of ecosystems. *Journal of Applied Remote Sensing*, 1, 1 - 21.

Asner G.P., Nepstad D., Cardinot G. & Ray D. (2004). Drought stress and carbon uptake in an Amazon forest measured with spaceborne imaging spectroscopy. *Proceedings of the National Academy of Sciences of the United States of America*, 101, 6039-6044.

Asner G.P. & Vitousek P.M. (2005). Remote analysis of biological invasion and biogeochemical change. *Proceedings of the National Academy of Sciences of the United States of America*, 102, 4383-4386.

Basedow R.W., Carmer D.C. & Anderson M.E. (1995). HYDICE system: Implementation and performance In: *SPIE Proceedings* Orlando, FL, USA.

Blundell A.G. & Peart D.R. (2004). Density-dependent population dynamics of a dominant rain forest canopy tree. *Ecology*, 85, 704-715.

Boardman J.W., Kruse F.A. & Green R.O. (1995). Mapping target signatures via partial unmixing of AVIRIS data. In: *Summaries of the fifth JPL airborne Earth science workshop*.

Brokaw N.V.L. (1982). The definition of treefall gap and its effect on measures of forest dynamics. *Biotropica*, 14, 158 - 160.

Brokaw N.V.L. (1985). Gap-phase regeneration in a tropical forest. *Ecology*, 66, 682-687.

Carlson K.M., Asner G.P., Hughes R.F., Ostertag R. & Martin R.E. (2007). Hyperspectral remote sensing of canopy biodiversity in Hawaiian lowland rainforests. *Ecosystems*, 10, 536-549.

Castro-Esau K.L., Sanchez-Azofeifa G.A., Rivard B., Wright S.J. & Quesada M. (2006). Variability in leaf optical properties of Mesoamerican trees and the potential for species classification. *American Journal of Botany*, 93, 517-530.

Caswell H. (2000). *Matrix population models: construction, analysis, and interpretation*. 2 edn.

Cavaleri M.A., Oberbauer S.F. & Ryan M.G. (2006). Wood CO_2 efflux in a primary tropical rain forest. *Global Change Biology*, 12, 2242 - 2458.

Cavaleri M.A., Oberbauer S.F. & Ryan M.G. (2008). Foliar and ecosystem respiration in an old-growth tropical rain forest. *Plant, Cell and Environment*.

Chambers J.Q., Asner G.P., Morton D.C., Anderson L.O., Saatchi S.S., Espirito-Santo F.D.B., Palace M. & Souza C. (2007). Regional ecosystem structure and function: ecological insights from remote sensing of tropical forests. *Trends in Ecology & Evolution*, 22, 414-423.

Chazdon R.L. (1988). Sunflecks and their importance to forest understory plants. *Advances in Ecological Research*, 18, 1-63.

Chazdon R.L. (1991). The importance of sunflecks for forest understory plants. *Bioscience*, 41, 760-766.

Chesson P.L. & Warner R.R. (1981). Environmental variability promotes coexistence in lottery competitive systems. *American Naturalist*, 117, 923-943.

Clark D.A. (2004). Sources or sinks? The responses of tropical forests to current and future climate and atmospheric composition. *Philosophical Transactions of the Royal Society of London Series B-Biological Sciences*, 359, 477-491.

Clark D.A. & Clark D.B. (1992). Life-history diversity of canopy and emergent trees in a Neotropical rain-forest. *Ecological Monographs*, 62, 315 - 344.

Clark D.A. & Clark D.B. (2001). Getting to the canopy: Tree height growth in a neotropical rain forest. *Ecology*, 82, 1460-1472.

Clark D.A., Piper S.C., Keeling C.D. & Clark D.B. (2003). Tropical rain forest tree growth and atmospheric carbon dynamics linked to interannual temperature variation during 1984-2000. *Proceedings of the National Academy of Sciences of the United States of America*, 100, 5852-5857.

Clark D.B., Castro C.S., Alvarado L.D.A. & Read J.M. (2004a). Quantifying mortality of tropical rain forest trees using high-spatial-resolution satellite data. *Ecology Letters*, 7, 52-59.

Clark D.B. & Clark D.A. (2000). Landscape-scale variation in forest structure and biomass in a tropical rain forest. *Forest Ecology and Management*, 137, 185 - 198.

Clark D.B., Clark D.A. & Read J.M. (1998). Edaphic variation and the mesoscale distribution of tree species in a neotropical rain forest. *Journal of Ecology*, 86, 101-112.

Clark D.B., Clark D.A., Rich P.M., Weiss S. & Oberbauer S.F. (1996). Landscape scale evaluation of understory light and canopy structure: Methods and application in a neotropical lowland rain forest. *Canadian Journal of Forest Research-Revue Canadienne De Recherche Forestiere*, 26, 747-757.

Clark D.B., Olivas P.C., Oberbauer S.F., Clark D.A. & Ryan M.G. (2008). First direct landscape-scale measurement of tropical rain forest Leaf Area Index, a key driver of global primary productivity. *Ecology Letters*, 11, 163-172.

Clark D.B., Read J.M., Clark M.L., Cruz A.M., Dotti M.F. & Clark D.A. (2004b). Application of 1-M and 4-M resolution satellite data to ecological studies of tropical rain forests. *Ecological Applications*, 14, 61-74.

Clark M.L., Clark D.B. & Roberts D.A. (2004c). Small-footprint lidar estimation of sub-canopy elevation and tree height in a tropical rain forest landscape. *Remote Sensing of Environment*, 91, 68-89.

Clark M.L., Roberts D.A. & Clark D.B. (2005). Hyperspectral discrimination of tropical rain forest tree species at leaf to crown scales. *Remote Sensing of Environment*, 96, 375-398.

Condit R. (2002). Beta-diversity in tropical forest trees. *Science*, 295, 666-669.

Condit R., Ashton P.S., Baker P., Bunyavejchewin S., Gunatilleke S., Gunatilleke N., Hubbell S.P., Foster R.B., Itoh A., LaFrankie J.V., Lee H.S., Losos E., Manokaran N., Sukumar R. & Yamakura T. (2000). Spatial patterns in the distribution of tropical tree species. *Science*, 288, 1414 - 1418.

Condit R., Hubbell S.P. & Foster R.B. (1995). Mortality rates of 205 Neotropical tree and shrub species and the impact of a severe drought. *Ecological Monographs*, 65, 419-439.

Cormack R.M. (1964). Estimates of survival from sighting of marked animals. *Biometrika*, 51, 429 - 438.

Curran P., J. (1989). Remote sensing of foliar chemistry. *Remote Sensing of Environment*, 30, 271 - 278.

Darwin C. (1859). *The origin of species by means of natural selection, or, the preservation of favored races in the struggle for life*. 1993 Modern Library Edition edn. Random House, New York.

Dennison P.E. & Roberts D.A. (2003). Endmember selection for multiple endmember spectral mixture analysis using endmember average RMSE. *Remote Sensing of Environment*, 87, 123-135.

Denslow J.S. (1980). Gap partitioning among tropical rainforest trees. *Biotropica*, 12, 47-55.

Drake J.B., Dubayah R.O., Clark D.B., Knox R.G., Blair J.B., Hofton M.A., Chazdon R.L., Weishampel J.F. & Prince S.D. (2002a). Estimation of tropical forest structural characteristics using large-footprint lidar. *Remote Sensing of Environment*, 79, 305-319.

Drake J.B., Dubayah R.O., Knox R.G., Clark D.B. & Blair J.B. (2002b). Sensitivity of large-footprint lidar to canopy structure and biomass in a neotropical rainforest. *Remote Sensing of Environment*, 81, 378-392.

Drake J.B., Knox R.G., Dubayah R.O., Clark D.B., Condit R., Blair J.B. & Hofton M. (2003). Above-ground biomass estimation in closed canopy Neotropical forests using lidar remote sensing: factors affecting the generality of relationships. *Global Ecology and Biogeography*, 12, 147-159.

Espeleta J.F. & Clark D.A. (2007). Multi-scale variation in fine-root biomass in a tropical rain forest: A seven-year study. *Ecological Monographs*, 77, 377-404.

Fearnside P.M. (2000). Global warming and tropical land-use change: greenhouse gas emissions from biomass burning, decomposition and soils in forest conversion, shifting cultivation and secondary vegetation. *Climate Change*, 46, 115 - 158.

Foster R.B. & Brokaw N.V.L. (1996). Structure and history of the vegetation of Barro Colorado Island. In: *The ecology of a tropical forest: seasonal rhythms and long-term changes* (eds. Leigh EG, Rand AS & Windsor DM). Smithsonian Institution Press Washington, DC, pp. 67 - 82.

Frankie G.W. (1974). Comparative phenological studies of trees in tropical wet and dry forests in lowlands of Costa Rica. *Journal of Ecology*, 62, 881-919.

Freed L.A., Conant S. & Fleischer R.C. (1987). Evolutionary ecology and radiation of Hawaiian passerine birds. *Trends in Ecology & Evolution*, 2, 196 - 203.

Gause F.W. (1934). *The struggle for existence*. Hafner, New York.

Gelman A. (2006). Prior distributions for variance parameters in hierarchical models (Comment on Article by Brown and Draper). *Bayesian Analysis*, 1, 515 - 534.

Gelman A. & Rubin D.B. (1992). Inference from iterative simulation using multiple sequences. *Statistical Science*, 7, 457 - 472.

Gilbert B., Wright S.J., Muller-Landau H.C., Kitajima K. & Hernandez A. (2006). Life history trade-offs in tropical trees and lianas. *Ecology*, 87, 1281-1288.

Hanski I. (1998). Metapopulation dynamics. *Nature*, 396, 41 - 49.

Hardesty B.D., Hubbell S.P. & Bermingham E. (2006). Genetic evidence of frequent long-distance recruitment in a vertebrate-dispersed tree. *Ecology Letters*, 9, 516-525.

Harms K.E., Condit R., Hubbell S.P. & Foster R.B. (2001). Habitat associations of trees and shrubs in a 50-ha neotropical forest plot. *Journal of Ecology*, 89, 947-959.

Harms K.E., Wright S.J., Calderon O., Hernandez A. & Herre E.A. (2000). Pervasive density-dependent recruitment enhances seedling diversity in a tropical forest. *Nature*, 404, 493-495.

Harper J.L. (1977). *Population biology of plants*. Academic Press.

Hartshorn G.S. & Hammel B.E. (1994). Vegetation types and floristic patterns. In: *La Selva: ecology and natural history of a neotropical rain forest* (eds. McDade LA, Bawa KS, Hespenheide HA & Hartshorn GS). University of Chicago Press Chicago, pp. 79 - 89.

Hubbell S.P. (1979). Tree dispersion, abundance, and diversity in a tropical dry forest. *Science*, 203, 1299-1309.

Hubbell S.P. (2001). *The unified neutral theory of biodiversity and biogeography*. Princeton University Press, Princeton, NJ.

Hubbell S.P. & Foster R. (1986a). Biology, chance, and history and the structure of tropical rain forest tree communities. In: *Community Ecology* (eds. Diamond JM & Case TJ). Harper and Rowe New York, pp. 314 - 329.

Hubbell S.P. & Foster R. (1986b). Canopy gaps and the dynamics of a neotropical forest. In: *Plant ecology* (ed. Crawley MJ). Blackwell Scientific Publications Oxford, pp. 77 - 96.

Hubbell S.P., Foster R.B., O'Brien S.T., Harms K.E., Condit R., Wechsler B., Wright S.J. & de Lao S.L. (1999). Light-gap disturbances, recruitment limitation, and tree diversity in a neotropical forest. *Science*, 283, 554-557.

Hubbell S.P., He F.L., Condit R., Borda-De-Agua L., Kellner J. & Ter Steege H. (2008). How many tree species are there in the Amazon and how many of them will go extinct? *Proceedings of the National Academy of Sciences of the United States of America*, in press.

Jablonski D., Roy K. & Valentine J.W. (2006). Out of the tropics: evolutionary dynamics of the latitudinal diversity gradient. *Science*, 314, 102.

Janzen D.H. (1967). Synchronozation of sexual reproduction of trees within dry season in Central America. *Evolution*, 21, 620-&.

Janzen D.H. (1970). Herbivores and the number of tree species in tropical forests. *The American Naturalist*, 104, 501 - 528.

Jolly G.M. (1965). Explicit estimates from capture-recapture data with both death and immigration-stochastic model. *Biometrika*, 52, 225 - 247.

Jones F.A., Chen J., Weng G.J. & Hubbell S.P. (2005). A genetic evaluation of seed dispersal in the neotropical tree Jacaranda copaia (Bignoniaceae). *American Naturalist*, 166, 543-555.

Kellner J.R., Clark D.B., Hofton M.A. & Dubayah R.O. (unpublished manuscript). Canopy and ground elevation in a mixed land use lowland Neotropical rain forest landscape.

Kennedy L.M. & Horn S.P. (2008). A late Holocene pollen and charcoal record from La Selva biological station, Costa Rica. *Biotropica*, 40, 11-19.

Kitajima K. & Hogan K.P. (2003). Increases of chlorophyll a/b ratios during acclimation of tropical woody seedlings to nitrogen limitation and high light. *Plant Cell and Environment*, 26, 857-865.

Kleber M., Schwendenmann L., Veldkamp E., Rößner J. & Reinhold J. (2007). Halloysite versus gibbsite: Silicon cycling as a pedogenetic process in two lowland neotropical rain forest soils of La Selva, Costa Rica. *Geoderma*, 138, 1 - 11.

Landis R.M. & Peart D.R. (2005). Early performance predicts canopy attainment across life histories in subalpine forest trees. *Ecology*, 86, 63-72.

Lunn D.J., Thomas A., Best N. & Spiegelhalter D. (2000). WinBUGS - A Bayesian modelling framework: Concepts, structure, and extensibility. *Statistics and Computing*, 10, 325-337.

MacArthur R. & Levins R. (1967). The limiting similarity, convergence, and divergence of coexisting species. *The American Naturalist*, 101, 377 - 385.

Martin M.E., Plourde L.C., Ollinger S.V., Smith M.L. & McNeil B. (2008). A generalizable method for remote sensing of canopy nitrogen across a wide range of forest ecosystems. In.

McGill B.J., Enquist B.J., Weiher E. & Westoby M. (2006). Rebuilding community ecology from functional traits. *Trends in Ecology & Evolution*, 21, 178 - 185.

Nelson B.W., Kapos V., Adams J.B., Oliveira W.J. & Braun O.P.G. (1994). Forest disturbance by large blowdowns in the Brazilian Amazon. *Ecology*, 75, 853 - 858.

Ollinger S.V. (2005). Net primary production and canopy nitrogen in a temperate forest landscape: An analysis using imaging spectroscopy, modeling and field data. *Ecosystems*, 8, 760-778.

Paine R.T. (1969). A note on trophic complexity and community stability. *American Naturalist*, 103, 91 - 93.

Porder S., Asner G.P. & Vitousek P.M. (2005). Ground-based and remotely sensed nutrient availability across a tropical landscape. *Proceedings of the National Academy of Sciences of the United States of America*, 102, 10909-10912.

Porder S., Clark D.A. & Vitousek P.M. (2006). Persistence of rock-derived nutrients in the wet tropical forests of La Selva, Costa Rica. *Ecology*, 87, 594-602.

Powell R.L., Roberts D.A., Dennison P.E. & Hess L.L. (2007). Sub-pixel mapping of urban land cover using multiple endmember spectral mixture analysis: Manaus, Brazil. *Remote Sensing of Environment*, 106, 253-267.

Pradel R. (1996). Utilization of capture-mark-recapture for the study of recruitment and population growth rate. *Biometrics*, 52, 703-709.

Reich P.B., Walters M.B. & Ellsworth D.S. (1997). From tropics to tundra: Global convergence in plant functioning. *Proceedings of the National Academy of Sciences of the United States of America*, 94, 13730-13734.

Roberts D.A., Gardner M., Church R., Ustin S., Scheer G. & Green R.O. (1998). Mapping chaparral in the Santa Monica Mountains using multiple endmember spectral mixture models. *Remote Sensing of Environment*, 65, 267-279.

Royle J.A. (2008). Modeling individual effects in the Cormack-Jolly-Seber model: a state-space formulation. *Biometrics*.

Saleska S.R., Didan K., Huete A.R. & da Rocha H.R. (2007). Amazon forests green-up during 2005 drought. *Science*, 318, 612.

Sanford R.L., Braker H.E. & Hartshorn G.S. (1986). Canopy openings in a primary neotropical lowland forest. *Journal of Tropical Ecology*, 2, 277 - 282.

Sanford R.L., Paaby P., Luvall J.C. & Phillips E. (1994). Climate, geomorphology, and aquatic systems. In: *La Selva: ecology and natural history of a neotropical rain forest* (eds. McDade LA, Bawa KS, Hespenheide HA & Hartshorn GS). University of Chicago Press Chicago, pp. 19 - 33.

Schat H., Vooijs R. & Kuiper E. (1996). Identical major gene loci for heavy metal tolerances that have independently evolved in different local populations and subspecies of *Silene vulgaris*. *Evolution*, 50, 1888 - 1895.

Seber G.A.F. (1965). A note on multiple-recapture census. *Biometrika*, 52, 249 - 259.

Sezen U., Chazdon R.L. & Holsinger K.E. (2007). Multigenerational genetic analysis of tropical secondary regeneration in a canopy palm. *Ecology*, 88, 3065 - 3075.

Smith M.L. (2002). Direct estimation of aboveground forest productivity through hyperspectral remote sensing of canopy nitrogen. *Ecological Applications*, 12, 1286-1302.

ter Steege H. (2006). Continental-scale patterns of canopy tree composition and function across Amazonia. *Nature*, 443, 444-447.

Tilman D. (1980). Resources: a graphical-mechanistic approach to competition and predation. *The American Naturalist*, 116, 362 - 393.

Treseder K.K. & Vitousek P.M. (2001). Potential ecosystem-level effects of genetic variation among populations of *Metrosideros polymorpha* from a soil fertility gradient in Hawaii. *Oecologia*, 126, 266 - 275.

Turchin P. & Taylor A.D. (1992). Complex population dynamics in ecological time-series. *Ecology*, 73, 289-305.

Ustin S.L., Roberts D.A., Gamon J.A., Asner G.P. & Green R.O. (2004). Using imaging spectroscopy to study ecosystem processes and properties. *Bioscience*, 54, 523-534.

Vitousek P.M. (2004). *Nutrient cycling and limitation: Hawai'i as a model system*. Princeton University Press, Princeton, NJ.

Wallace A.R. (1878). *Tropical nature and other essays*. Macmillan, London.

Webb C.O. & Peart D.R. (2000). Habitat associations of trees and seedlings in a Bornean rain forest. *Journal of Ecology*, 88, 464-478.

Wood T.E., Lawrence D. & Clark D.A. (2005). Variation in leaf litter nutrients of a Costa Rican rain forest is related to precipitation. *Biogeochemistry*, 73, 417-437.

Wright S.J. & Calderon O. (2006). Seasonal, El Nino and longer term changes in flower and seed production in a moist tropical forest. *Ecology Letters*, 9, 35-44.

Wright S.J., Muller-Landau H.C., Calderon O. & Hernandez A. (2005). Annual and spatial variation in seedfall and seedling recruitment in a neotropical forest. *Ecology*, 86, 848-860.

Young T.P. & Hubbell S.P. (1991). Crown asymmetry, treefalls, and repeat disturbance of broad-leaved forest gaps. *Ecology*, 72, 1464-1471.

Zhang J.K. (2006). Intra and inter-class spectral variability of tropical tree species at La Selva, Costa Rica: Implications for species identification using HYDICE imagery. *Remote Sensing of Environment*, 105, 129-141.

Zimmerman J.K., Wright S.J., Calderon O., Pagan M.A. & Paton S. (2007). Flowering and fruiting phenologies of seasonal and aseasonal neotropical forests: the role of annual changes in irradiance. *Journal of Tropical Ecology*, 23, 231-251.